united nations
educational, scientific
and cultural
organization

international atomic
energy agency

the
abdus salam
international centre for theoretical physics

SMR.1348 - 11

SECOND EUROPEAN SUMMER SCHOOL on MICROSCOPIC QUANTUM MANY-BODY THEORIES and their APPLICATIONS

(3 - 14 September 2001)

THE NUCLEAR MANY-BODY PROBLEM

Stefano FANTONI
S.I.S.S.A.
Via Beirut 2-4
I-34014 Trieste
ITALY

The Nuclear Many–Body Problem

Stefano Fantoni
International School for Advanced Studies, SISSA
International Centre for Theoretical Physics, ICTP

ICTP, September 2001, Trieste

SISSA

1. Introduction

2. Nuclear Hamiltonian

3. AFDMC: a new QMC method

4. EOS of nucleon matter

5. Droplets

6. Spin susceptibility of neutron matter

7. Conclusion and perspectives

Kevin Schmidt (Tempe, Arizona)
Antonio Sarsa (SISSA)
Adelchi Fabrocini (Pisa)

1. - Introduction

Nucleon Matter $\rightarrow$ Heavy nuclei $\rightarrow$ Light nuclei

(a) Equation of state $\rightarrow \frac{E}{A}(\rho, T, J_z)$

- $N = Z$
- Neutron Matter
- $N \neq Z$

(b) Single particle properties $\rightarrow$ Shell model

- $e(k)$, $n(k)$ and $n(e)$
- Self–energy and Optical Potential

(c) Response functions $\rightarrow$ Inclusive reactions

(d) Spectral functions $\rightarrow$ Semi–exclusive reactions

(e) Magnetic properties, $\cdots$

$(\downarrow)$ $\cdots$

(∞) Standard model of nuclear physics

Why nucleon matter ?

The Mass Formula

$$\frac{E}{A} = -a_v + a_\tau \frac{(Z-N)^2}{A^2} + \frac{a_s}{A^{1/3}} + a_C \frac{Z^2}{A^{4/3}} + \frac{\delta_p}{A^{7/4}}$$

where

$$\begin{aligned} a_v &= \sim 16MeV \\ a_\tau &= \sim 30MeV \\ a_s &= \sim 19MeV \\ a_C &= 0.717MeV \\ \delta_p &= 0,\ \pm 34MeV \\ \rho(r=0) &\rightarrow \rho_0 = 0.17fm^{-3} \end{aligned}$$

Fermi gas

$$
\begin{aligned}
k_F &= \left(\frac{6\pi^2\rho_0}{d}\right)^{1/3} = 1.36 fm^{-1} \\
\epsilon_F(k) &= \frac{\hbar^2 k^2}{2m} \\
T_F &= 38.35 MeV \\
\frac{< T >_F}{A} &= \frac{3\hbar^2 k_F^2}{10m} = 23.01 MeV \\
a_\tau^F &= \sim 27 Mev \\
n_F(k) &= \theta(k - k_F) \\
P_h^F(k, E) &= n_F(k)\delta(E - \frac{\hbar^2 * k^2}{2m})
\end{aligned}
$$

Add N–N interaction $\rightarrow$ N–N correlations

$\downarrow$

$\downarrow$

Nucleon systems are strongly correlated many–body systems.

1. $< T > /A : \sim 23 MeV \rightarrow \sim 45 MeV$

2. depletion of the occupation of orbits $\rightarrow \sim 75\%$

3. suppression of single particle contributions $\rightarrow Z \sim 0.65$

4. semi–inclusive electron scattering reactions at intermediate energies

5. .....

(e,e') reactions

CBF theory

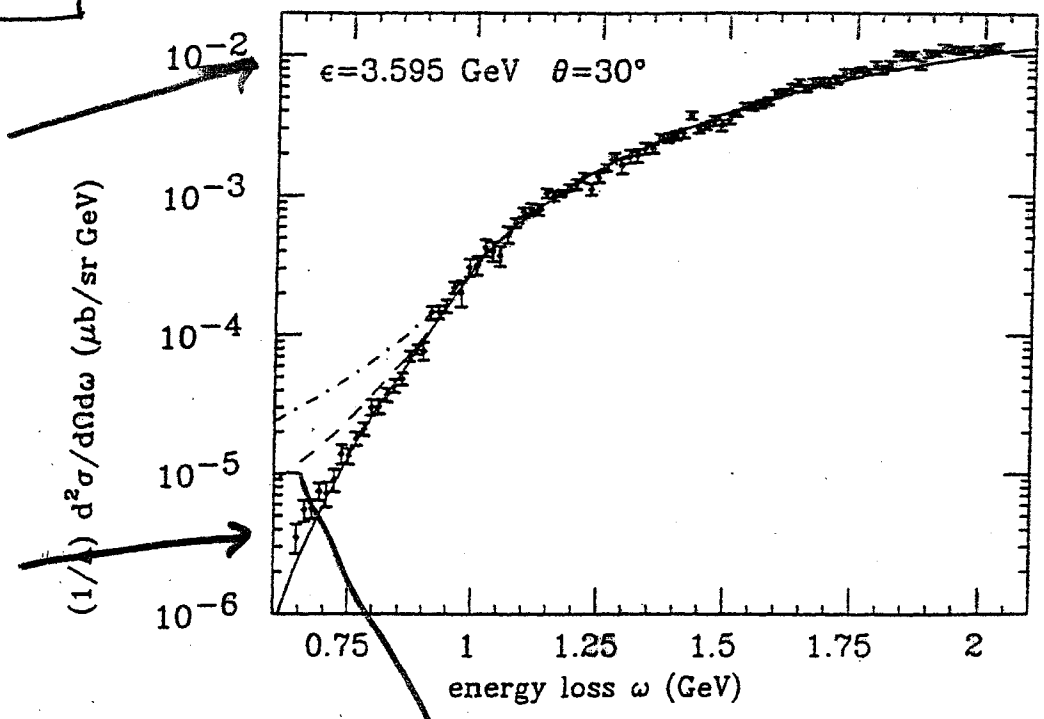

FIG. 5. Calculated cross section for incident electron energy $\epsilon=3.595$ GeV and scattering angle $\theta=30°$, compared with the experimental data. The dot-dashed and the dashed lines correspond to the results obtained with F_L and F_G, respectively. The solid line is obtained with $F_{\rm QCT}$.

$$\Phi[z=v(q)t]\equiv\exp\left[-i(V-iW)\frac{z}{\hbar v(q)}\right]. \tag{3.13}$$

The eikonal approximation,

$$\Phi(z)=\exp\left[\frac{-i}{\hbar v(q)}\int_0^z d\xi\, v_{\rm int}(\xi)\right], \tag{3.14}$$

is used to calculate $\Phi(z)$ and the q and t dependent optical potential V and W in Eq. (3.13). This approximation is valid if the quantity $v_{\rm int}\Phi$ varies slowly within distances of the order of $1/q$ and if $v_{\rm int}/E_q \ll 1$. The $v_{\rm int}(\xi)$ represents the interaction of all the nucleons with the struck nucleon and it is taken as

$$v_{\rm int}=\sum_i v_{{\rm eff},q}(\mathbf{r}-\mathbf{r}_i), \tag{3.15}$$

where $\mathbf{r}_i$ denotes the positions of the other nucleons. The $v_{{\rm eff},q}$ is obtained from the free N-N scattering data as

$$v_{{\rm eff},q}(\mathbf{r})=-\frac{2\pi\hbar}{m}\int\frac{d\mathbf{k}}{(2\pi)^3}e^{i\mathbf{k}\cdot\mathbf{r}}f_q(\mathbf{k}), \tag{3.16}$$

where $f_q(\mathbf{k})$ is the amplitude for the scattering of a nucleon of momentum q, with momentum transfer $\mathbf{k}$, by free nucleons at rest.

If the ground-state correlations are neglected, Eq. (3.15) becomes

$$v_{\rm int}(\mathbf{r})=-\frac{2\pi\rho\hbar^2}{m}\int\frac{d\mathbf{k}}{(2\pi)^3}d\mathbf{r}'e^{i\mathbf{k}\cdot(\mathbf{r}-\mathbf{r}')}f_q(\mathbf{k})$$

$$=-\frac{2\pi\rho\hbar^2}{m}f_q(k=0). \tag{3.17}$$

Substituting this $v_{\rm int}(\mathbf{r})$ in Eq. (3.14), we get the trivial result

$$W(q)=\frac{2\pi\rho\hbar^2}{m}\Im(f_q(k=0))$$

$$=\frac{\hbar}{2}\rho v(q)\sigma_{NN}(q). \tag{3.18}$$

In order to include the effects of the correlations among the hole associated with the struck nucleon and the remaining nucleons, in first-order approximation, $v_{\rm int}(\mathbf{r})$ is given by

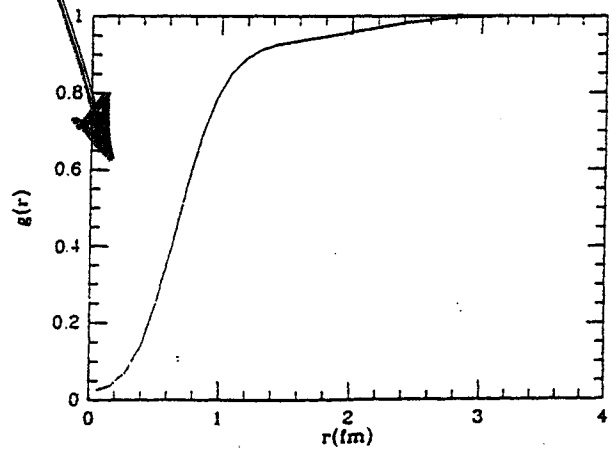

FIG. 6. Pair distribution function of nuclear matter at the empirical saturation density ($k_F=1.33$ fm^{-1}).

LDA theory

Spectral function P(k,E)

O. Benhar et al. / Nuclear matter

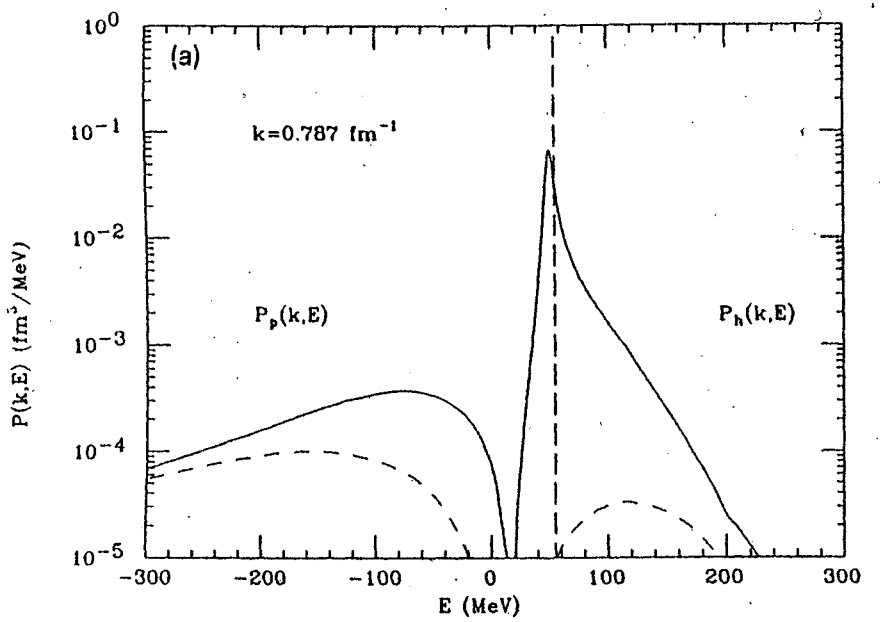

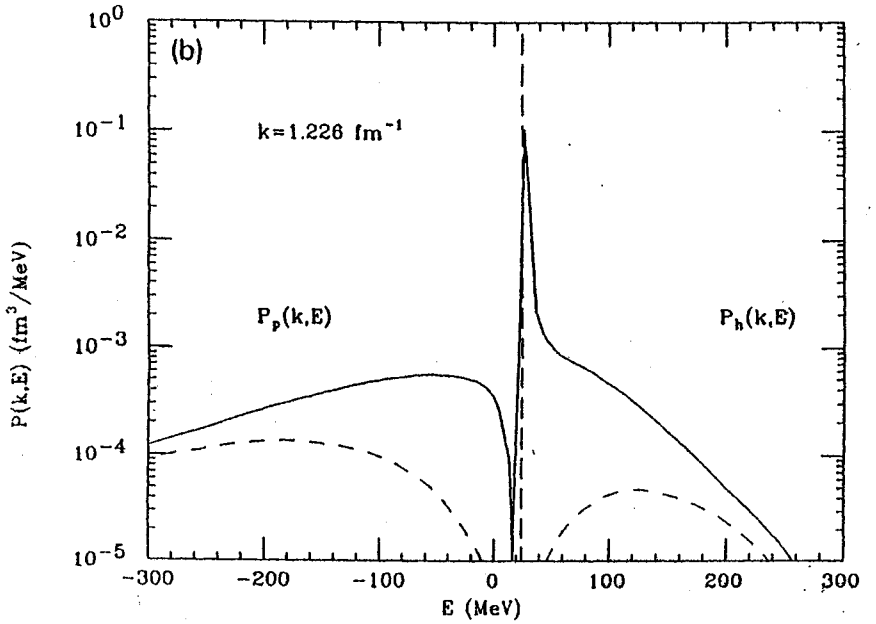

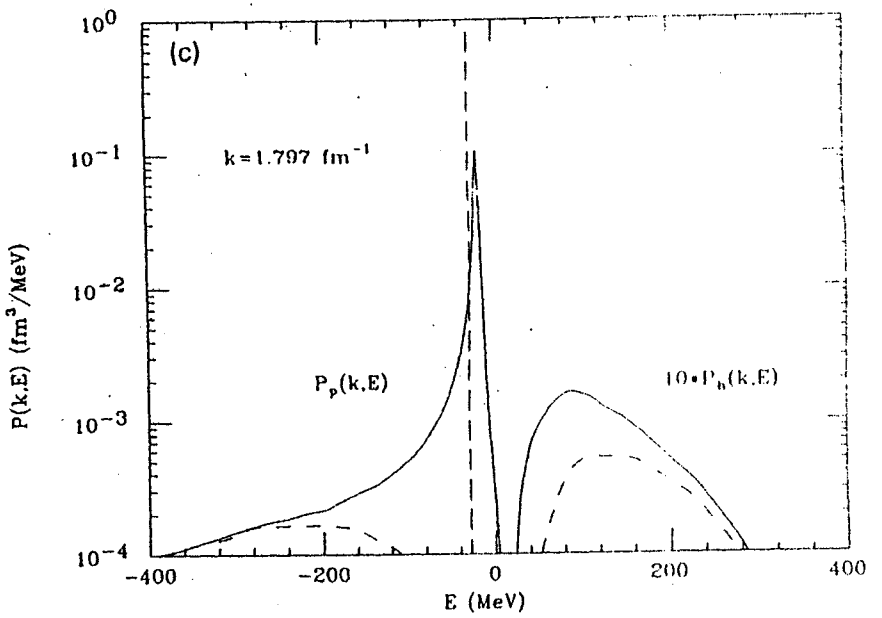

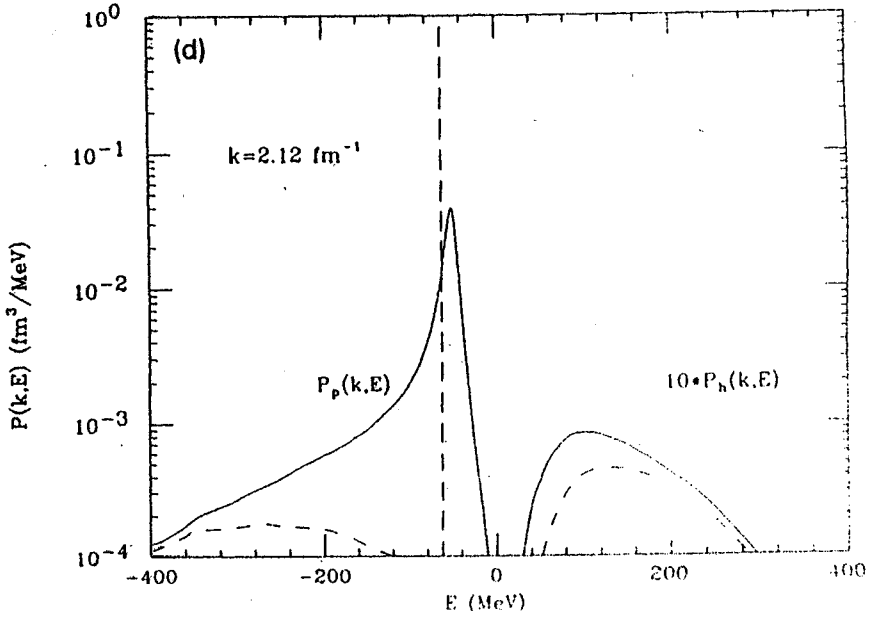

-8-

$$\int_{-e_v(k_F)}^{\bar{E}} dE\ P_h(k,E)$$

CBF-theory

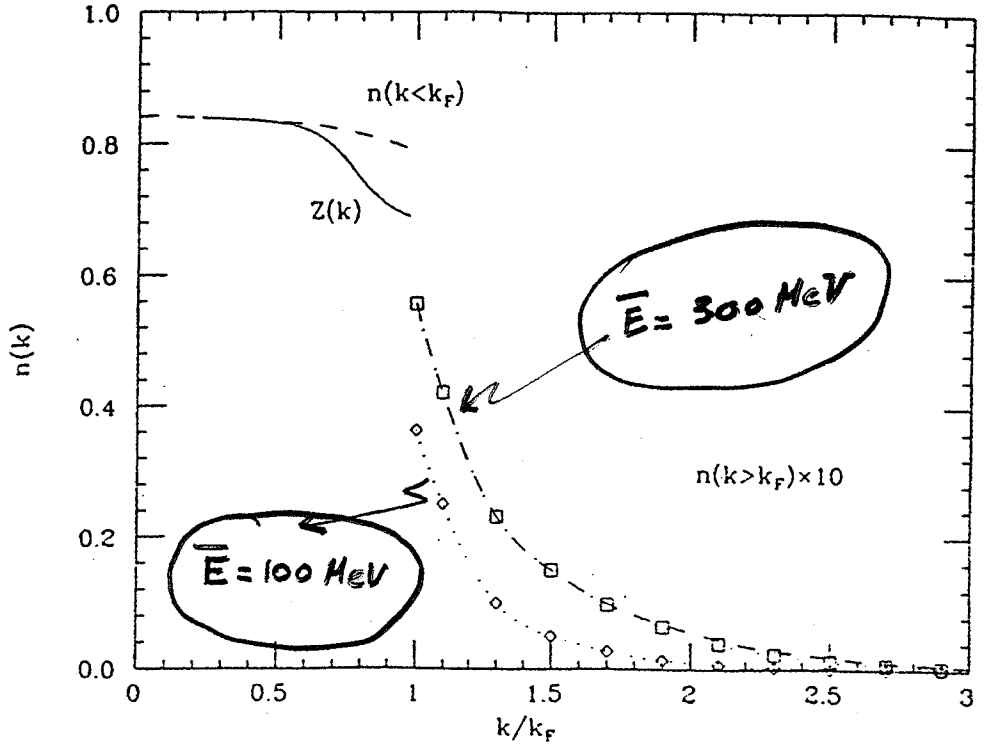

Fig. 6 *Removal energy integral of the nuclear spectral function* $n_{\bar{E}}(k) = \int_{-e_v(k_F)}^{\bar{E}} dE P(k,E)$ *in the CO-model of nuclear matter. The dotted lines with open diamonds and squares refer to* $\bar{E} = 100, 300 MeV$ *respectively. The solid line gives the quasi-hole strength* $Z(k)$*, whereas the dashed line is the full* $n(k)$*.*

$$P(k,E) = \frac{1}{\pi} \mathrm{Im} \frac{\langle 0 | a_k^+ (H - E_0 - E - i\eta)^{-1} a_k | 0 \rangle}{\langle 0 | 0 \rangle}$$

$$\int dE\ P(k,E) = n(k) = \frac{\langle 0 | a_k^+ a_k | 0 \rangle}{\langle 0 | 0 \rangle}$$

Momentum distribution of liquid ^{3}He

Fixed node - DMC

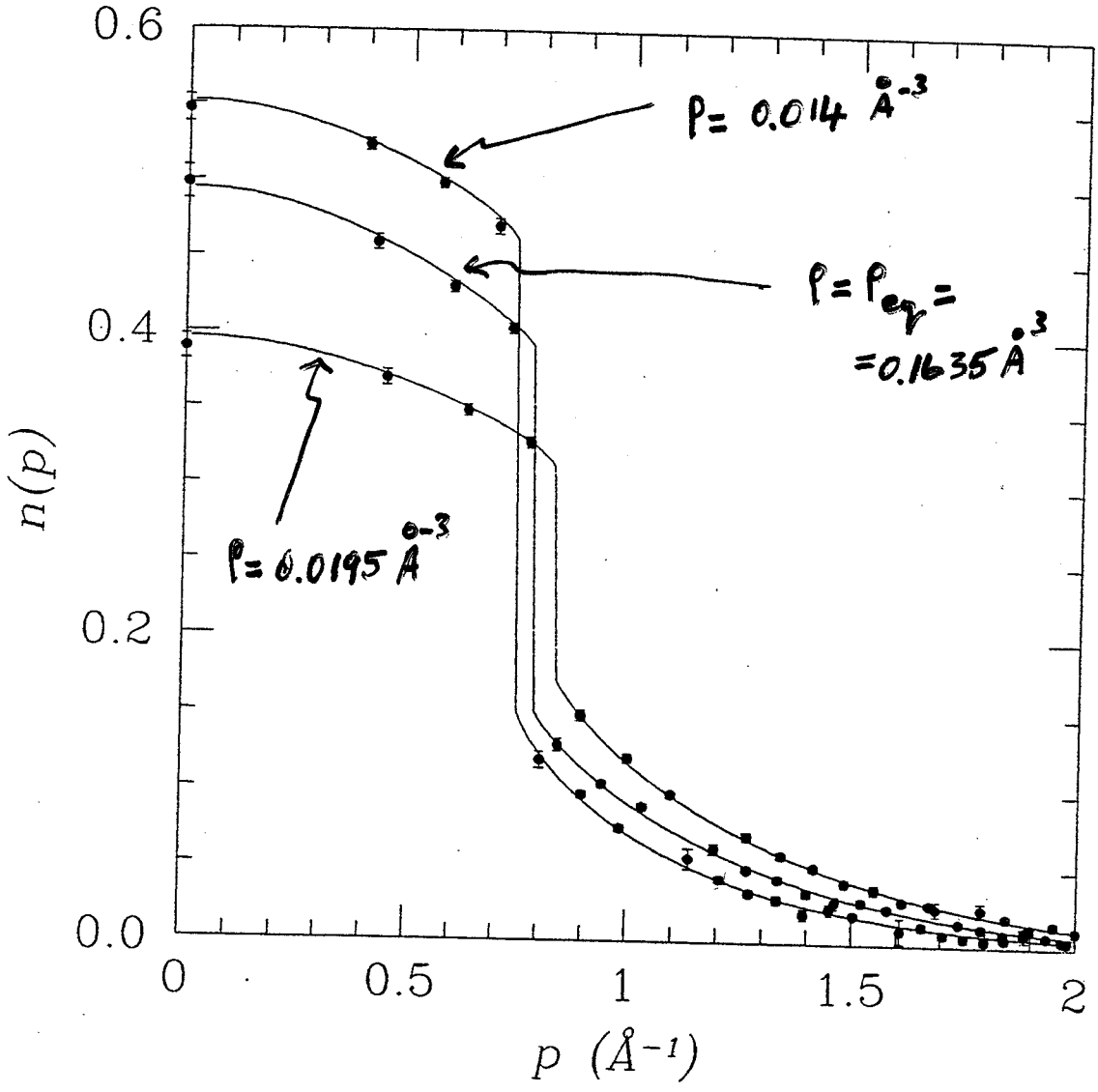

Symmetric nuclear matter: FHNC/SOC results

Argonne v_{18} two–body potential
+ Urbana IX three–body interaction †

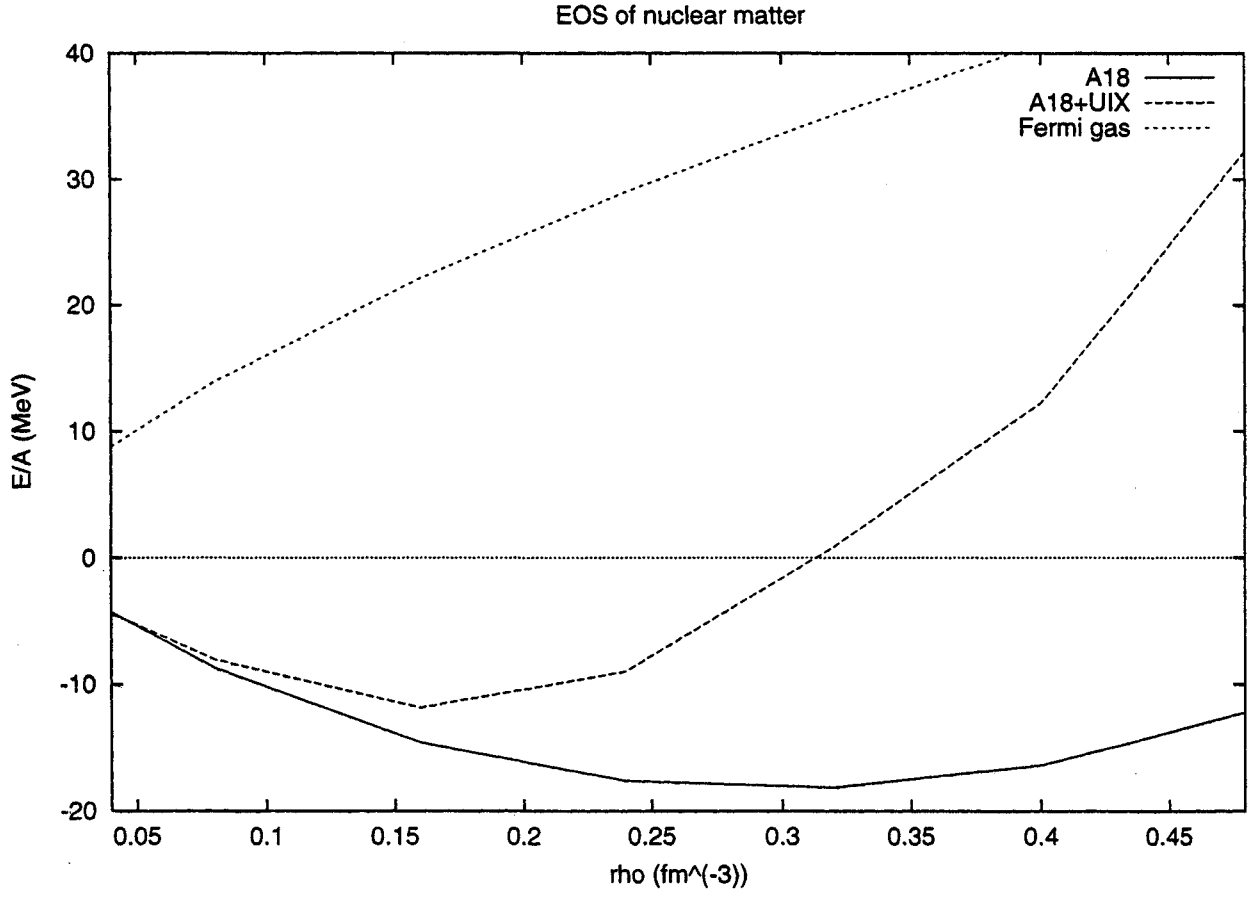

†A.Akmal et al., Phys. Rev. **C58**, (1998) 1804

Pure neutron matter: FHNC/SOC results

Argonne v_{18} two–body potential plus UIX
old Argonne v_{14} two–body interaction plus UVII[‡]

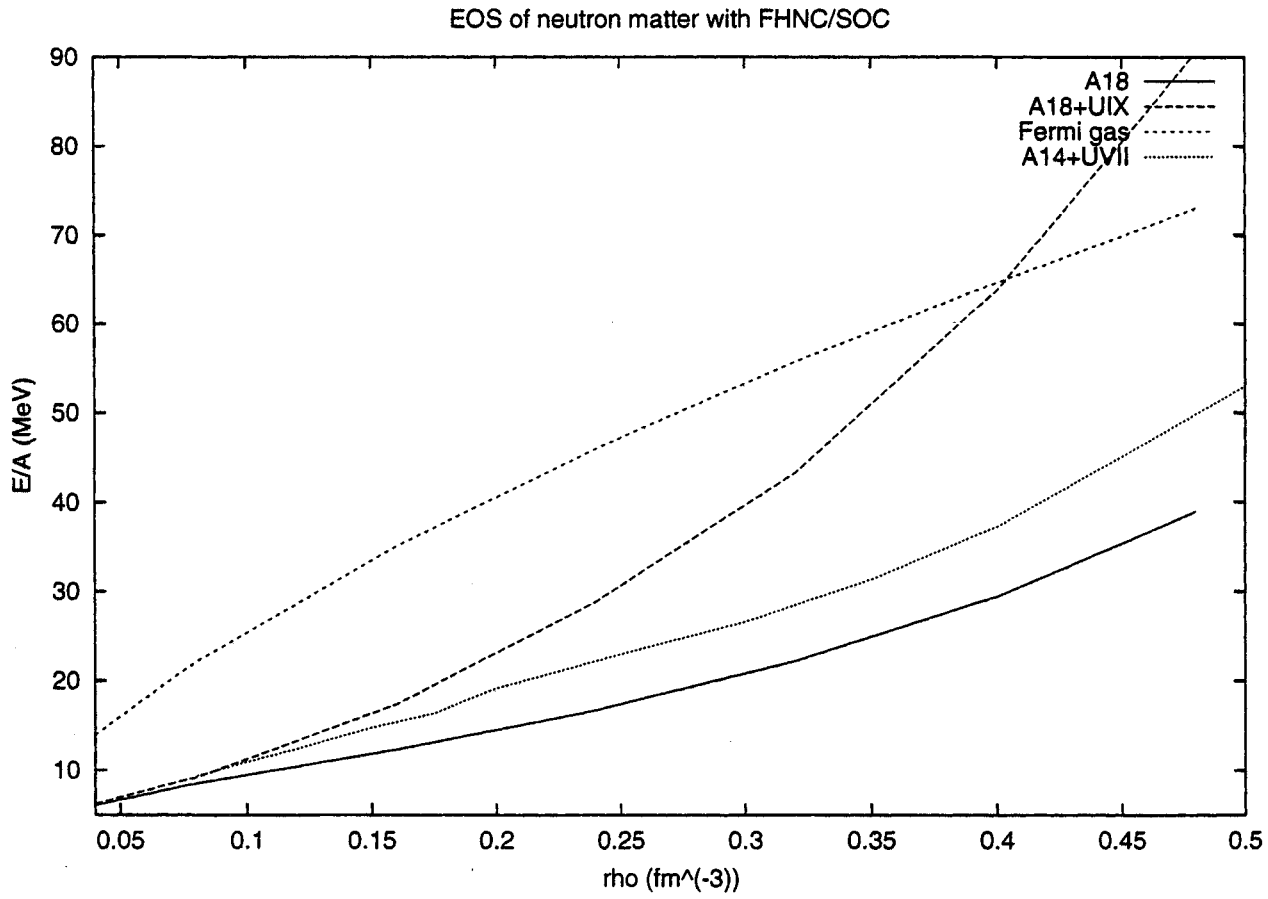

[‡]R.B.Wiringa, V.Ficks and A.Fabrocini, Phys. Rev. **C38** (1988) 1010

Existing Many–body methods

- Correlated Basis Function, ...
  - Bridge diagrams
    Are they important in nucleon systems ?
  - Spin problem
    Need to go beyond SOC approximation ?
  - Perturbation theory
    is second order enough ?
  - N $\neq$ Z, spin polarization, finite T

- Brueckner Hartree–Fock, ...
  - convergence problems
  - many–body forces

- Quantum Simulations : standard GFMC
  - limits on the size of the nucleon system ($A \leq 10$).

Pure neutron matter: FHNC/SOC versus BHF[§]

Argonne v_{18} two–body potential plus UIX
old Argonne v_{14} two–body interaction plus UVII

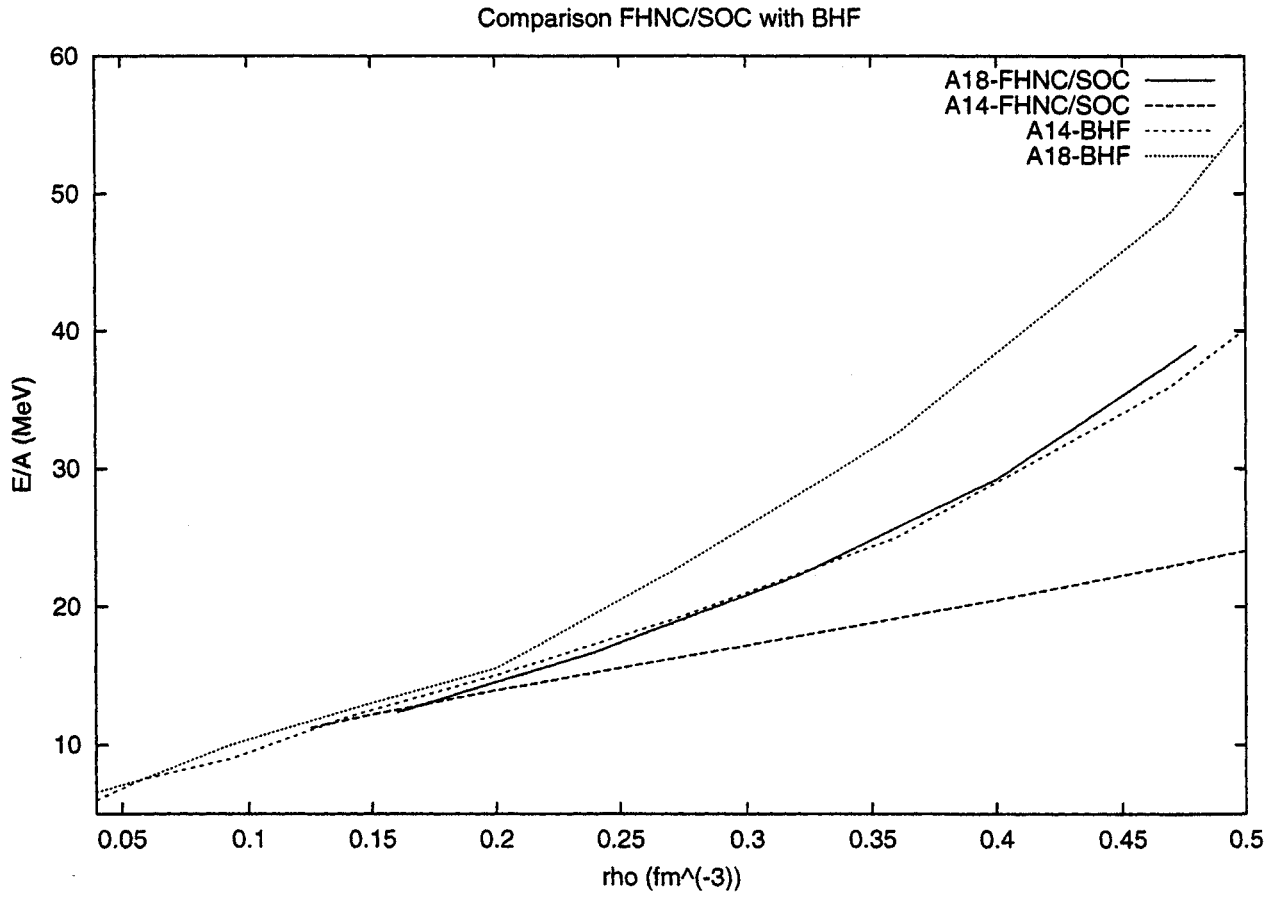

[§]M.Baldo, I.Bombaci and G.F.Burgio, Astr. Astrophys. 328 (1997) 274
L.Engwick et al., Nucl. Phys. **A627** (1997) 85

Spin problem

The nuclear hamiltonian is strongly spin–isospin–dependent

1. CBF theory

   (a) Spin–dependent correlations $\rightarrow$ Commutators problem
   (b) Jastrow correlations $\rightarrow$ convergence of CBF

2. Stochastic methods

   (a) $D \neq D\uparrow \times D\downarrow$ as in liquid ^{3}He
   D is a $4N \times 4N$ complex matrix
   (b) complete summation over the spin–isospin states
   (c) sample the spin–isospin states

Standard GFMC[¶]

The spin–independent part of the nucleon hamiltonian can be handled using standard GFMC or DMC

Standard GFMC uses Monte Carlo for central part and complete summation over the spin-isospin states.

The number of good S_z T_z spin-isospin states is

$$\frac{A!}{Z!(A-Z)!}2^A$$

which can be lowered by a small factor if good T^2 states are constructed.

The exponential growth of these states limits this brute force method to $A <\approx 10$

[¶]R.B. Wiringa, S.C. Pieper, J. Carlson and V.R.Pandharipande, Phys. Rev **C62**, 2000

2. - Nuclear Hamiltonian

1. Non relativistic models

   (a) Modern two–nucleon interactions
   (b) Three–nucleon interaction
   (c) Consistent nucleon currents
   (d) relativistic corrections

2. Relativistic many–body models

3. Other degrees of freedom ?

   (a) Meson and Deltas
   (b) Born–Oppenheimer approximation
   (c) short–range interaction

Non relativistic Hamiltonian

$$
\begin{aligned}
H &= T + V_2 + V_3 \\
&= -\frac{\hbar^2}{2m} \sum_{i=1,N} \nabla_i^2 + \sum_{i<j} v_{ij} + \sum_{i<j<k} V_{ijk}
\end{aligned}
$$

Urbana–Argonne form

$$
\begin{aligned}
v_l &= \sum_{i<j} v_{ij} = \sum_{i<j} \sum_{p=1}^{l} v_p(r_{ij}) O^p(i,j) \\
O^{p\leq 8} &\rightarrow \left(1, \vec{\sigma}_i \cdot \vec{\sigma}_j, S_{ij}, \frac{1}{2}\vec{L}_{ij} \cdot (\vec{\sigma}_i + \vec{\sigma}_j)\right) \otimes (1, \vec{\tau}_i \cdot \vec{\tau}_j) \\
S_{ij} &= 3(\hat{r}_{ij} \cdot \vec{\sigma}_i)(\hat{r}_{ij} \cdot \vec{\sigma}_j) - \vec{\sigma}_i \cdot \vec{\sigma}_j \\
\vec{L}_{ij} &= \frac{1}{2i}(\vec{r}_i - \vec{r}_j) \times (\vec{\nabla}_i - \vec{\nabla}_j)
\end{aligned}
$$

$v_l(r)$ $\leftarrow$ one–pion exchange plus a phenomenological shorter range part

Argonne v_{18} two–body potential†

This potential includes:

- 8 standard components
- other 6 charge independent terms
  $(L^2,\ L^2\ \vec{\sigma}_i \cdot \vec{\sigma}_j,\ (\vec{L} \cdot \vec{S})^2) \otimes (1, \vec{\tau}_i \cdot \vec{\tau}_j)$
- plus '4 charge–symmetry–breaking and charge–dependent components.
- It fits both pp and np scattering data up to 350 MeV (**Nijmegen database**) with a $\chi^2/datum \sim 1$.

Modern two–body potentials $\equiv \chi^2/datum \sim 1$
Argonne v_{18}, Reid-93, Nijmegen-I and II, CD-Bonn

---

†S.C. Pieper, V.R. Pandharipande, R.B.Wiringa and J. Carlson, Phys. Rev. **C64**, 2001

A simplified two–body potential: The Argonne v_8' potential[‡]

$\downarrow$

- a new fit of to the N–N data
- it equals the isoscalar part of v_{18} in all S and P waves as well as in the $^3D_1$ wave and its coupling to the $^3S_1$
- it has been used in GFMC calculations on light nuclei, and in FHNC/SOC calculations on nuclear matter
- differences with the v_{18} potential can be safely estimated in a perturbative way

Pure neutron matter $\rightarrow \quad \vec{\tau_i} \cdot \vec{\tau_j} = 1$

[‡]B.S. Pudliner et al. , Phys. Rev. **C56**, 1720 (1997)

Table 1: The GFMC energies (in MeV) of the ground states of stable nuclei with $A \leq 8$ computed with Argonne v_{18} and v_8' two–body interactions are compared with experimental data.

nucleus	$A8'$	$A18$	$Expt$
^{3}H	-7.76(1)	-7.61(1)	-8.48
^{3}He	-7.02(1)	-6.87(1)	-7.72
^{4}He	-25.14(2)	-24.07(4)	-28.30
^{6}He	-25.20(6)	-23.9(1)	-29.27
^{6}Li	-28.19(5)	-26.9(1)	-31.99
^{7}Li	-33.56(6)	-31.6(1)	-39.24
^{8}He	-23.8(1)	-21.6(2)	-31.41
^{8}Li	-34.2(1)	-31.8(3)	-41.28
^{8}Be	-47.9(1)	-45.6(3)	-56.50
^{7}n	-33.78(4)	-33.47(5)	
^{8}n	-39.73(6)	-39.21(8)	

Neutron matter: BHF2 results for modern N–N two–body interactions[§]

Modern two–nucleon interactions
Argonne v_8' with AFDMC and 14 neutrons

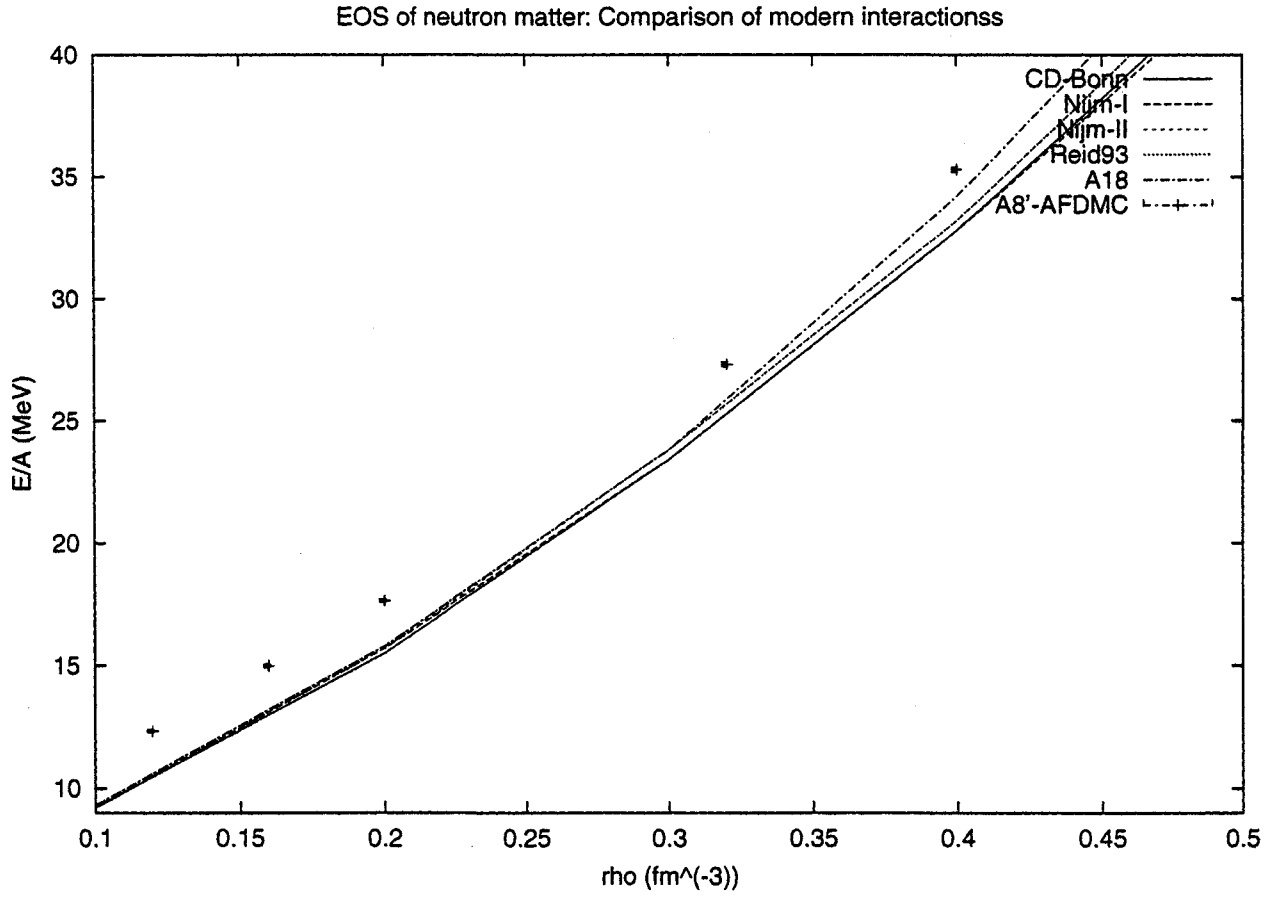

[§]L.Engvik, et al. Nucl.Phys. **A627** (1997) 85

Neutron matter: Comparison of different calculations

Argonne v_{18} two–nucleon interaction
Argonne v_8' with AFDMC and 14 neutrons

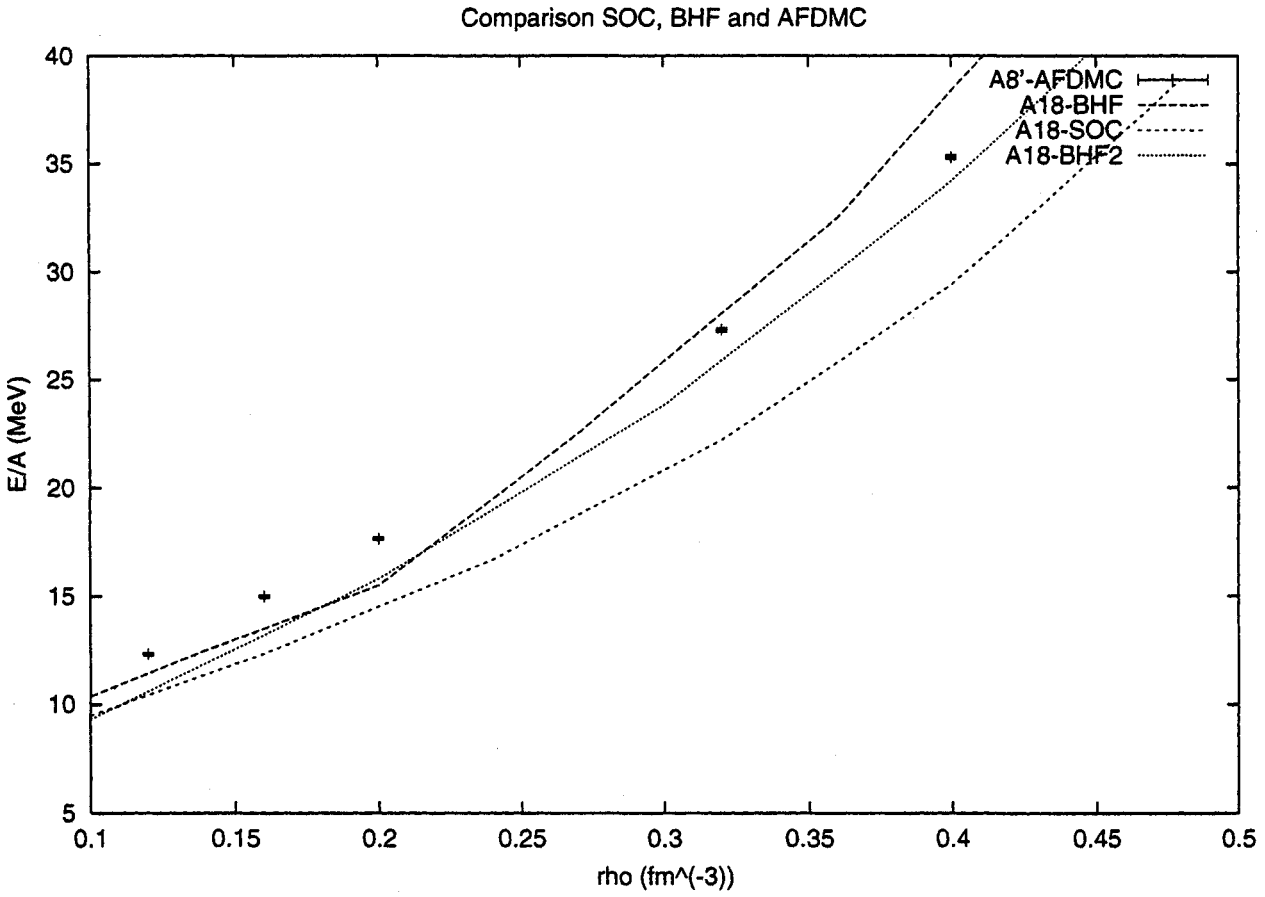

Three–body interaction: Illinois scheme[¶]

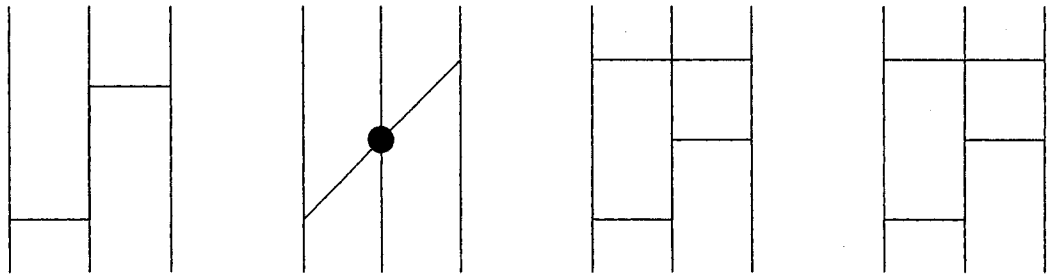

red line $\rightarrow$ π
blue line $\rightarrow$ Δ

$$V_{ijk}^{UIX} = A_{2\pi}^{PW} O_{ijk}^{2\pi,PW} + A_R O_{ijk}^R$$
$$V_{ijk} = V_{ijk}^{UIX} + A_{2\pi}^{SW} O_{ijk}^{2\pi,SW} + A_{3\pi}^{\Delta R} O_{ijk}^{3\pi,\Delta R}$$

[¶]Steven C. Pieper, et al, Phys. Rev. **C64** (2001) 14001

- $O_{ijk}^{2\pi,PW}$ → Fujita–Miyazawa term → Diagram A
- O_{ijk}^{R} → Repulsive phenomenological term
- $O_{ijk}^{2\pi,SW}$ → S-wave term → Diagram B
- $O_{ijk}^{3\pi,\Delta R}$ → three–pion terms → Diagrams C and D

$$O_{ijk}^{R} = \sum_{cyclic} T^2(m_\pi, c_3; r_{ik}) T^2(m_\pi, c_3; r_{kj}) \ ,$$

$$\begin{aligned} Y(x) &= \frac{e^{(}-x)}{x}\chi(r) \\ T(x) &= \left(\frac{3}{x^2}+\frac{3}{x}+1\right) Y(x)\chi(r) \\ \chi(r) &= (1-e^{-c_3 r^2}) \end{aligned}$$

Four fitting parameters plus the cut–off parameter c_3

Urbana IX for Neutron Matter

For neutrons, the Urbana-IX interaction is given by the sum of a spin independent and a spin dependent part

$$V_{ijk} = V_{ijk}^{SI} + V_{ijk}^{SD}$$

$$\downarrow$$

$$\begin{aligned} V_{ijk}^{SI} &= U_0 \sum_{cyclic} T^2(m_\pi, c_3; r_{ik}) T^2(m_\pi, c_3; r_{kj}) \ , \\ V_{ijk}^{SD} &= B_{2\pi} \sum_{cyclic} \{X_{ik}^\pi, X_{kj}^\pi\} \end{aligned}$$

$$\downarrow$$

$$X_{ik}^\pi = Y(m_\pi, c_3; r_{ik}) \vec{\sigma}_i \cdot \vec{\sigma}_k + T(m_\pi, c_3; r_{ik}) S_{ik}$$

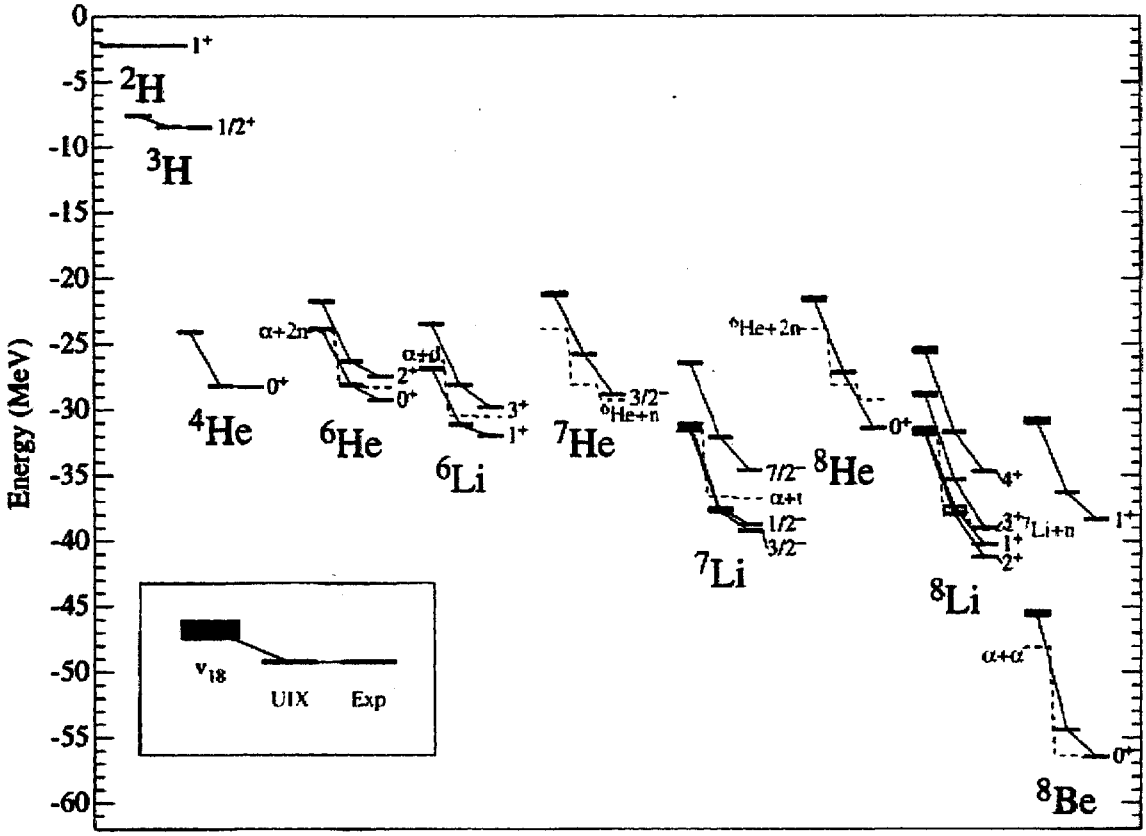

FIG. 1. (Color) Energies of ground or low-lying excited states of light nuclei computed with the AV18 and AV18/UIX interactions, compared to experiment. The light shading shows the Monte Carlo statistical errors. The dashed lines indicate the thresholds against breakup for each model or experiment.

tion of the spectrum of light nuclei. Studies of nuclear and neutron star matter with these new models will be reported in a separate paper.

The theory of strong interactions has not yet progressed enough to permit a first-principles determination of the two- and three-nucleon interactions with the accuracy required to calculate nuclear binding energies. The interactions must be determined phenomenologically. Modern, realistic models of v_{ij} are obtained by fitting the ~4300 data below 350 MeV in the Nijmegen NN-scattering database [6] with a $\chi^2 \sim 1$ per degree of freedom. The Nijmegen database is said to be complete, i.e., the included data determine all the relevant phase shifts and mixing parameters. Thus v_{ij} fitted to it are well determined and generally give very similar predictions of the properties of three- and four-body nuclei, as will be discussed below.

In contrast it is much more difficult to construct realistic models of V_{ijk} by simply fitting three-nucleon scattering data, which is dominated by the pairwise forces. The number of operators that can contribute to V_{ijk} is very large, and until recently, the number of observables that could both be observed and accurately calculated was small. Recent advances in three-nucleon scattering calculations, based on correlated hyperspherical harmonic [7] and Faddeev [8] methods, and in high-precision Nd scattering experiments, hold significant promise for testing models of V_{ijk} in this regime. However, the binding energies and excitation spectra of light nuclei also contain a great deal of information, and are in fact the only current means to investigate $T=3/2$ forces.

An additional concern is that the V_{ijk} obtained by fitting nuclear data may depend strongly on the model of v_{ij} used in the Hamiltonian. The V_{ijk} will naturally depend upon the chosen v_{ij} to some extent. For example, two equivalent models of v_{ij}, related by a unitary transformation, will have different but related V_{ijk} associated with them [9]. However, combinations of v_{ij} and V_{ijk} related by unitary transformations will naturally predict the same observables.

Models of V_{ijk} based on the elimination of field variables date back to the work of Primakoff and Holstein [10]. The first modern meson-exchange model for nuclear V_{ijk} was proposed by Fujita and Miyazawa (FM) [11]; it contained only the two-pion-exchange three-nucleon interaction $V^{2\pi,PW}$ due to scattering of the pion being exchanged between two nucleons by a third nucleon via the P-wave Δ resonance. This interaction is attractive in nuclei and nuclear matter. Later theoretical models, such as Tucson-Melbourne (TM) [12] and Brazil [13] included the $V^{2\pi,SW}$ due to πN S-wave scattering and $V^{2\pi,PW}$ from all P-wave scattering. In the recent Texas model, these two-pion-exchange contribu-

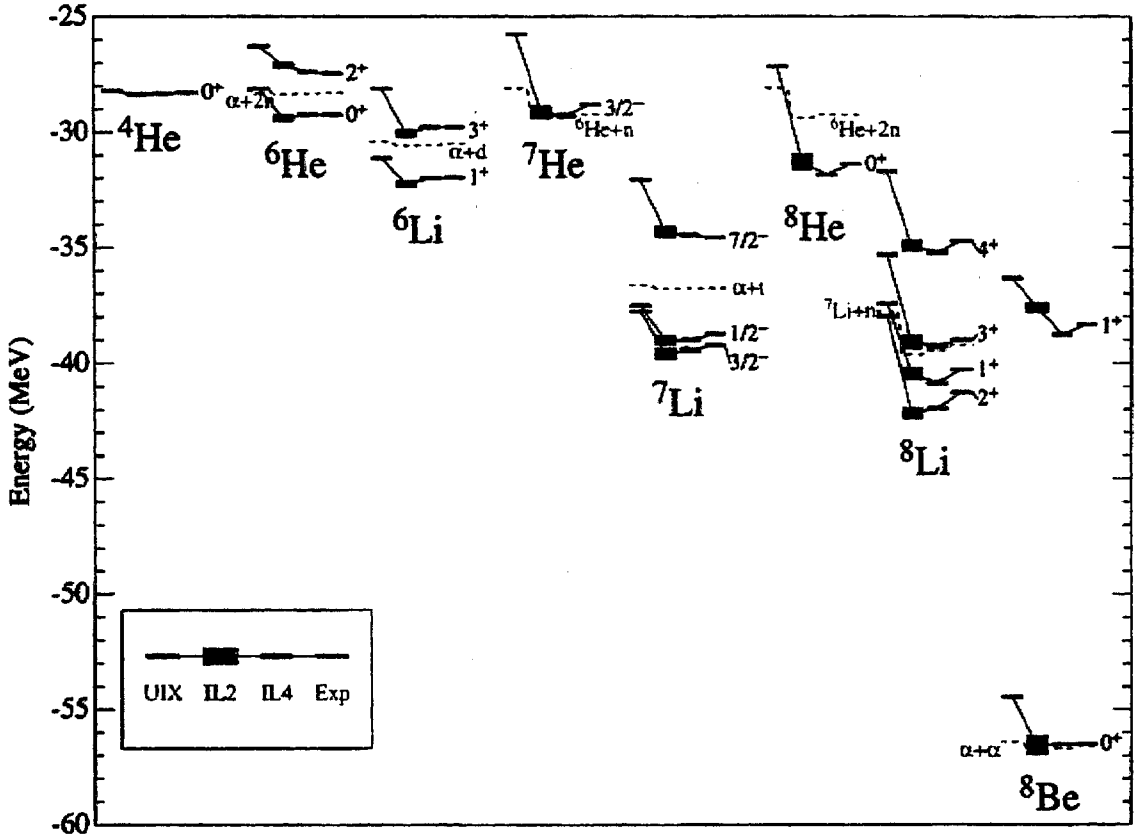

FIG. 3. (Color) Energies computed with the AV18/UIX, AV18/IL2, and AV18/IL4 Hamiltonians compared to experiment for narrow states. The light shading shows the Monte Carlo statistical errors. The dashed lines indicate the thresholds against breakup for each model or experiment.

of ^{8}Be. More quantitatively, Tables III and IV show various averages of the deviations from experiment for the narrow states of Table II. Table III is based on the deviations of the total energies of the 17 states, while Table IV is based on the deviations of the excitation energies of excited states. Both tables show the average deviation (which includes the signs of the deviations), the average of the magnitudes of the deviations, and the rms deviations. The average deviations in Table III demonstrate that the Hamiltonians with no V_{ijk} systematically underbind these nuclei by 5 to 7 MeV; AV18/UIX reduces this to the still large value of 2 MeV underbinding. The five Illinois models have no significant systematic under or overbinding. Because the errors for the AV8′, AV18, and AV18/UIX cases are so one-sided, their average

TABLE III. Average deviations (in MeV) from experimental energies. For each Hamiltonian, the average signed deviation, average magnitude of deviation, and rms deviation are shown for the 17 "narrow" states given in Table II (only ^{3}He energies are used for $A=3$).

Model	Average deviation	Average |deviation|	rms deviation
AV8′	5.52(2)	5.52	5.83
AV18	7.32(5)	7.32	7.72
AV18/UIX	2.02(4)	2.02	2.34
AV18/IL1	−0.09(6)	0.31	0.38
AV18/IL2	−0.10(6)	0.28	0.36
AV18/IL3	0.04(7)	0.31	0.44
AV18/IL4	−0.21(6)	0.24	0.33
AV18/IL5	−0.12(6)	0.34	0.46

TABLE IV. Average deviations (in MeV) from experimental excitation energies for the eight "narrow" excited states. As in Table III, but for excitation energies rather than total energies.

Model	Average deviation	Average |deviation|	rms deviation
AV8′	−0.23(5)	0.83	1.20
AV18	−0.22(10)	0.90	1.36
AV18/UIX	0.17(8)	0.41	0.53
AV18/IL1	0.29(13)	0.44	0.53
AV18/IL2	0.53(12)	0.53	0.61
AV18/IL3	0.03(14)	0.24	0.34
AV18/IL4	0.09(12)	0.20	0.25
AV18/IL5	0.27(13)	0.66	0.79

Neutron matter: Comparison of different three–body potentials

The two–body interaction is Argonne v_8'
AFDMC method with 14 neutrons

Three–body potentials : UIX, IL-2, IL-4

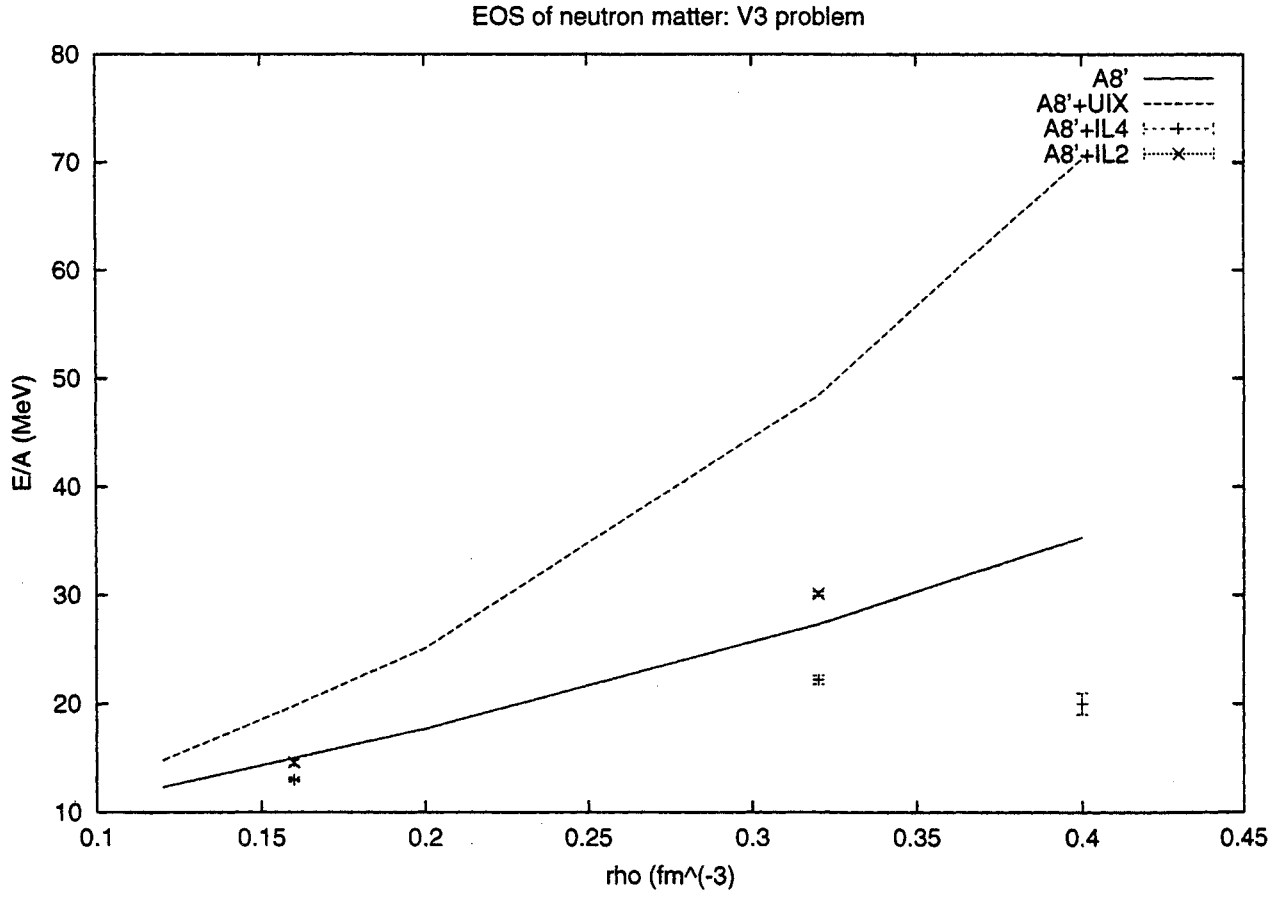

? Homework problem ?

Model interaction

1. Argonne v_6' potential ($A6'$)
2. Argonne v_8' potential ($A8'$)
3. Argonne v_8' potential plus UIX three–body interaction ($AU8'$)

Systems of interest

1. ^{4}He, ^{16}O, ^{40}Ca
2. symmetrical nuclear matter up to $2\rho_0$
3. ^{8}n with two single particle potentials
4. neutron matter up to $2\rho_0$

3. - AFDMC: Auxiliary Field Diffusion Monte Carlo for nucleon systems[1]

- AFDMC uses Auxiliary fields to linearize the spin–dependent part of the propagator
- AFDMC samples the spin states rather than making a complete sum
- AFDMC treats the spatial part of the $\Psi(R,S)$ as in DMC
- AFDMC allows for $N \neq Z$ and polarized systems
- AFDMC does both nucleon matter and nuclei
- AFDMC has already simulated 76 nucleons
- AFDMC scales in A as standard DMC.

[1] K.E.Schmidt, S.Fantoni, Phys. Lett. **B 446** (1999) 99

Auxiliary Field Motivation

- We need to sample the spin states to do large A systems.

- Past attempts to sample them in the S_z, T_z basis have failed.

- The S_z, T_z basis gives high variance – we want a basis where relatively few samples are a good representation of the wave function.

Let's look at a coherent state basis. In our code we use the usual spinors, but .... with coherent state basis ideas.

$$|\hat{\Omega}\rangle \equiv |\theta, \phi\rangle \equiv e^{-i\frac{\phi}{2}\sigma_z} e^{-i\frac{\theta}{2}\sigma_y} |\uparrow\rangle$$

A general spinor is $|\hat{\Omega}\rangle$ times a phase factor, and

$$\langle\hat{\Omega}|\vec{\sigma}|\hat{\Omega}\rangle = \hat{\Omega}\,.$$

Advantages of a Coherent State Basis

Two reasons for coherent state basis to give lower variance:

1. If we have a weak spin exchange or spin flip interaction, the spin state will be mostly the usual spin-independent result. The coherent state can smoothly add a small spin flip component.

2. We used the coherent state basis to introduce spin correlations in liquid helium, with results that were hindered only by the fermi sign problem.[1]

[1] J.W. Lawson, S.A. Vitiello, K.E. Schmidt, and S. Fantoni, Phys. Rev. Lett. **78**, 1846 (1997).

Disadvantage of Coherent State Basis

Coherent states are not orthogonal and overcomplete

$$\int \frac{d\Omega}{2\pi} |\hat{\Omega}\rangle\langle\hat{\Omega}| = 1$$

Even though operators like

$$\int \frac{d\Omega}{2\pi} |\hat{\Omega}\rangle F(\hat{\Omega})\langle\hat{\Omega}|$$

look diagonal, they are not. Even if $\hat{\Omega} \neq \hat{\Omega}'$

$$\langle\hat{\Omega}'|\hat{\Omega}\rangle \neq 0$$

Things like fixed node don't go through as simply as with an orthogonal basis.

Walking the Spinors

The spin independent term of the hamiltonian are treated as in standard DMC

We want to sample the states produced by the imaginary time propagator $\exp(-(V_2^{SD} + V_3^{SD})\Delta t)$

$$\Psi(X) = \int dX' G_0(R, R') e^{-V\Delta t + E_0 \Delta t} P_{LS} \Psi(X')$$

$$G_0(R, R') = \left(\frac{m}{2\pi\hbar^2\Delta t}\right)^{3/2} \exp\left(-\frac{m|R - R'|^2}{2\hbar^2\Delta t}\right)$$

where $X \equiv R, S$ denotes the new positions, and X' the old ones.

Walking the Spinors: continue

(a) We want our propagation to be local. That is: as $\Delta t \to 0$ we want our propagator to go smoothly to the identity and the walker to remain the same.

(b) One way is to write the spin part of the propagator as

$$\sum_{\text{samples}} \prod_{i=1}^{A} [a_i + \vec{b}_i \cdot \vec{\sigma}_i][c_i + \vec{d}_i \cdot \vec{\tau}_i]$$

(c) The Hubbard-Stratonovich or auxiliary field method accomplishes this breakup

The Hubbard-Stratonovich or auxiliary field method

Consider a two–particle system

$$\begin{aligned}
&\exp(-\sigma_{x1}\sigma_{x2}v_{12}^{\sigma}\Delta t) \\
&= \cosh(v_{12}^{\sigma}\Delta t)[1-\sigma_{x1}\sigma_{x2}\tanh(v_{12}^{\sigma}\Delta t)] \\
&= \cosh(v_{12}^{\sigma}\Delta t)\frac{1}{2}\sum_{\epsilon=\pm 1}\left[1+\epsilon\sigma_{x1}\sqrt{\tanh(-v_{12}^{\sigma})}\right] \\
&\left[1+\epsilon\sigma_{x2}\sqrt{\tanh(-v_{12}^{\sigma})}\right]
\end{aligned}$$

As $\Delta t \to 0$ this goes smoothly to 1, and for nonzero Δt, the spinors each get multiplied by a near unit 2×2 matrix. The ϵ variables are sampled using the Monte Carlo method.

The breakup above requires 3 Hubbard-Stratonovich variables for each pair of particles for a spin-exchange and tensor interaction, or $3A(A-1)/2$ variables.

Our Breakup: v_6 interaction

To reduce the number of HS variables we diagonalize V^{SD} in spin–isospin space. This requires Order(A^3) operations, but the trial wave function determinant has the same complexity.
$\rightarrow$ This breakup is similar to those used in auxiliary field break ups in Shell Model Monte Carlo.

$$
\begin{aligned}
V &= \sum_{i<j}[\sum_{p=1}^{6} v_p(r_{ij})O^{(p)}(i,j)] = V_c + V_{nc} \\
&= V_c + \frac{1}{2}\sum_{i,\alpha,j,\beta} \sigma_{i,\alpha} A^{(\sigma)}_{i,\alpha,j,\beta} \sigma_{j,\beta} \\
&+ \frac{1}{2}\sum_{i,\alpha,j,\beta} \sigma_{i,\alpha} A^{(\sigma\tau)}_{i,\alpha,j,\beta} \sigma_{j,\beta} \vec{\tau}_i \cdot \vec{\tau}_j \\
&+ \frac{1}{2}\sum_{i,j} A^{(\tau)}_{i,j} \vec{\tau}_i \cdot \vec{\tau}_j
\end{aligned}
$$

1. Our A matrices are zero when $i = j$ and symmetric.

2. All the A matrices are real and symmetric
   $\rightarrow$ real eigenvalues and eigenvectors.

$$\sum_{j,\beta} A^{(\sigma)}_{i,\alpha,j,\beta} \vec{\psi}^{\sigma}_{n}(j) \cdot \hat{x}_{\beta} = \lambda^{(\sigma)}_{n} \vec{\psi}^{\sigma}_{n}(i) \cdot \hat{x}_{\alpha}$$

3. The matrices can be written in terms of their eigenvectors and eigenvalues

$$\begin{aligned} V^{SD} &= \frac{1}{2} \sum_{i,j,n} \vec{\sigma}_i \cdot \vec{\psi}^{(\sigma)}_{n}(i) \lambda^{(\sigma)}_{n} \vec{\psi}^{(\sigma)}_{n}(j) \cdot \vec{\sigma}_j \\ &+ \frac{1}{2} \sum_{i,j,n} \vec{\sigma}_i \cdot \vec{\psi}^{(\sigma\tau)}_{n}(i) \lambda^{(\sigma\tau)}_{n} \vec{\psi}^{(\sigma\tau)}_{n}(j) \cdot \vec{\sigma}_j \vec{\tau}_i \cdot \vec{\tau}_j \\ &+ \frac{1}{2} \sum_{i,j,n} \vec{\tau}_i \cdot \vec{\tau}_j \psi^{(\tau)}_{n}(i) \lambda^{(\tau)}_{n} \psi^{(\tau)}_{n}(j) \end{aligned}$$

One more step to get the squares of operators

$$
\begin{aligned}
V^{SD} &= \frac{1}{2}\sum_{n=1}^{3A}(O_n^{(\sigma)})^2\lambda_n^{(\sigma)} \\
&+ \frac{1}{2}\sum_{\alpha=1}^{3}\sum_{n=1}^{3A}(O_{n\alpha}^{(\sigma\tau)})^2\lambda_n^{(\sigma\tau)} \\
&+ i\frac{1}{2}\sum_{\alpha=1}^{3}\sum_{n=1}^{A}(O_{n\alpha}^{(\tau)})^2\lambda_n^{(\tau)}
\end{aligned}
$$

with

$$
\begin{aligned}
O_n^{(\sigma)} &= \sum_i \vec{\sigma}_i \cdot \vec{\psi}_n^{(\tau)}(i) \\
O_{n\alpha}^{(\sigma\tau)} &= \sum_i \tau_{i\alpha}\vec{\sigma}_i \cdot \vec{\psi}_n^{(\sigma\tau)}(i) \\
O_{n\alpha}^{(\tau)} &= \sum_i \tau_{i\alpha}\psi_n^{(\tau)}(i)
\end{aligned}
$$

The Hubbard Stratonovich transformation

$$e^{-\frac{1}{2}\lambda_n O_n^2 \Delta t} = \left(\frac{\Delta t|\lambda_n|}{2\pi}\right)^{\frac{1}{2}} \int_{-\infty}^{\infty} dx e^{-\frac{1}{2}\Delta t|\lambda_n|x^2 - \Delta t s \lambda_n O_n x}$$

where s is 1 for $\lambda < 0$, and i for $\lambda > 0$.

(A) Our O_n don't commute, so we need to keep the time steps small so that the commutator terms can be ignored. Each of the O_n is a sum of 1-body operators as required above.

(B) A discrete version of this transformation is given by[2]

$$\begin{aligned} e^{-\frac{1}{2}\lambda_n O_n^2 \Delta t} &= \int_{-\infty}^{\infty} dx f(x) e^{-\Delta t s \lambda_n O_n x} + \mathrm{O}(\Delta t^3) \\ f(x) &= \frac{1}{6}\left[\delta(x-h) + 4\delta(x) + \delta(x+h)\right] \end{aligned}$$

[2] S. E. Koonin, D. J. Dean, and K. Langanke, Phys. Rept. **278**, 1 (1997)

(C) the value of h is given by

$$h = \left(\frac{3}{|\lambda_n|\Delta t}\right)^{\frac{1}{2}}.$$

one can use a more accurate formula (5,7, .. points) or gaussian distribution

(D) We require 3A Hubbard-Stratonovich variables for the σ terms, $9A$ variables for the $\sigma\tau$ terms, and $3A$ variables for the τ terms. Each time step requires the diagonalization of two $3A$ by $3A$ matrices and one A by A matrix.

(E) Many other breakups are possible.

Spin rotation - Neutron matter

$$e^{-\frac{1}{2}\lambda_n O_n^2 \Delta t} = \left(\frac{\Delta t|\lambda_n|}{2\pi}\right)^{\frac{1}{2}} \int_{-\infty}^{\infty} dx e^{-\frac{1}{2}\Delta t|\lambda_n|x^2 - \Delta t s \lambda_n O_n x}$$

- We sample a value of x_n for the n-th field variable
- We make a rotation in the spin space:

R: S' $\rightarrow$ S

Rotate the spin state of each individual particle k

$$|\eta'_k >= a'_k| \uparrow > + b'_k| \downarrow > \rightarrow |\eta_k >$$

$\lambda_n \leq 0$:

$$\begin{aligned}
\eta_k &= \hat{R}\,\eta'_k \\
\eta'_k &= a'_k|\uparrow> + b'_k|\downarrow> \\
\eta_k &= a_k|\uparrow> + b_k|\downarrow>
\end{aligned}$$

$$\begin{aligned}
a_k &= a'_k(\cosh(A_n) + \sinh(A_n)\psi_n^z(k)) \\
&+ b'_k \sinh(A_n)(\psi_n^x(k) - \imath\ \psi_n^y(k)) \\
b_k &= b'_k(\cosh(A_n) - \sinh(A_n)\psi_n^z(k)) \\
&+ a'_k \sinh(A_n)(\psi_n^x(k) + \imath\ \psi_n^y(k)) \\
A_n &= \Delta t|\lambda_n| x_n \sqrt{[(\psi_n^x(k))^2 + (\psi_n^y(k))^2 + (\psi_n^z(k))^2]}
\end{aligned}$$

$\lambda_n > 0$:

$$\sinh(A_n) \rightarrow \imath\ \sin(-A_n)$$

Three–body potential - Neutron Matter

The spin–dependent part of Urbana IX potential, reduces to a sum of terms containing only two-body spin operators

$$
\begin{aligned}
\{X^{\pi}_{ik}, X^{\pi}_{kj}\} &= 2\, x^{\mu\nu}_{ijk} \vec{\sigma}^{\mu}_{i} \vec{\sigma}^{\nu}_{j} \\
x^{\mu\nu}_{ijk} &= y_{ik} y_{kj} \delta_{\mu\nu} + y_{ik} t^{\mu\nu}_{kj} + t^{\mu\nu}_{ik} y_{kj} + t^{\mu\alpha}_{ik} t^{\alpha\nu}_{kj} \\
y_{ik} &= Y(m_{\pi}, c_3, r_{ik}) - T(m_{\pi}, c_3, r_{ik}) \\
t^{\mu\nu}_{ik} &= 3\, T(m_{\pi}, c_3, r_{ik}) \hat{r}^{\mu}_{ik} \hat{r}^{\nu}_{ik} \; .
\end{aligned}
$$

Incorporate the spin–dependent part of the three–body interaction V_3^{SD} in the matrix $A_{i,\alpha,j,\beta}$

$$
A_{i,\alpha,j,\beta} \rightarrow A_{i,\alpha,j,\beta} + 2 \sum_{k} B_{2\pi} x^{\alpha\beta}_{ijk} \; .
$$

The Spin-Orbit Propagator

Keep in the propagator all the terms linear on Δt
$\rightarrow$ two– and three–body, spin–dependent counter–terms.

$$(\vec{\nabla}_j - \vec{\nabla}_k) G_0(R, R') = \frac{-m}{\hbar^2 \Delta t} (\Delta \vec{r}_j - \Delta \vec{r}_k) G_0(R, R')$$

$$P_{LS} = \exp\left(\sum_{j \neq k} \frac{m v_{LS}(r_{jk})}{4 i \hbar^2} [(\vec{\sigma}_j + \vec{\sigma}_k) \times \vec{r}_{jk}] \cdot \Delta \vec{r}_j \right)$$

gives the correct term along with some extra incorrect contributions

Expand Ψ, and the propagator in powers of Δr and Δt, keeping all terms linear in Δt or quadratic in Δr.

$$V_2^{add} = -\sum_{j<k} \frac{m r_{jk}^2 v_{LS}^2(r_{jk})}{8\hbar^2}$$
$$[2 + \vec{\sigma}_j \cdot \vec{\sigma}_k - \vec{\sigma}_j \cdot \hat{r}_{jk} \vec{\sigma}_k \cdot \hat{r}_{jk}]$$
$$V_3^{add} = -\sum_{j<k<p \text{ cyclic}} \sum \frac{m r_{jk} r_{jp} v_{LS}(r_{jk}) v_{LS}(r_{jp})}{16\hbar^2}$$
$$\{\hat{r}_{jk} \cdot \hat{r}_{jp} [2 + \vec{\sigma}_k \cdot \vec{\sigma}_j + \vec{\sigma}_p \cdot \vec{\sigma}_j + \vec{\sigma}_k \cdot \vec{\sigma}_p]$$
$$-\vec{\sigma}_j \cdot \hat{r}_{jk} \vec{\sigma}_k \cdot \hat{r}_{jp} - \vec{\sigma}_p \cdot \hat{r}_{jk} \vec{\sigma}_j \cdot \hat{r}_{jp} - \vec{\sigma}_p \cdot \hat{r}_{jk} \vec{\sigma}_k \cdot \hat{r}_{jp}\}$$

Without the above counter–terms the extrapolated mixed and growth energies do not agree.

Constrained Path

- We still have the usual fermi sign problem. Here, the overlap of walkers with the trial function is complex (phase problem) .

- We constrain the path to regions where the real part of the overlap with our trial function is positive.

- For spin independent potentials this reduces to the fixed-node approximation.

- There is no real proof that AFDMC gives an upper bound

- Actual calculations suggest that AFDMC gives an upper bound

- In any case, one can use path integral techniques or forward walking to overcome this problem

Is it an Upper Bound ?

The original argument by Zhang et al. (now retracted ?) is essentially that the wave function goes continuously to zero at the node as Δt goes to zero, so the contribution from the node to H also goes to zero and the contribution of the true H and the effective constrained path H are the same everywhere else, so you can replace

$$\langle \Psi_T | H \exp(-H_{CP} t) | \Psi_T \rangle$$

with

$$\langle \Psi_T | \exp(-H_{CP} t/2) H \exp(-H_{CP} t/2) | \Psi_T \rangle$$

and get the same result.

Unfortunately, because of the nonorthogonality of the Coherent states, this argument does not go through, but it is suggestive.

Scaling with A

- We have not done a detailed analysis, but roughly it appears that our time step scales as A^{-1} from the eigenvalue range of our potential matrices. We have reduced this somewhat by using multiple small auxiliary field steps for each diagonalization.

- We found that a time step of $\Delta\tau = 10^{-4} MeV^{-1}$ is generally sufficient in neutron matter simulations to get consistency between the mixed and the growth energies up to $2\rho_0$ and 66 neutrons.

- The order A^3 diagonalizations are the same order as the fermion determinants, so they cost an overall prefactor to standard fermion Green's function Monte Carlo of perhaps a factor of 10 or 20.

Tail corrections

- Monte Carlo calculations are generally performed within the sphere of radius $L/2$

- Tail corrections are estimated by integrating out the spin–independent part of the two–body potential from $L/2$ up to ∞

- We use full simulation box, and, include also the contribution from the neighbor cells (26 are generally enough up to twice ρ_0)

$$F(\vec{r}) = \prod_{mno} f(|x_m\hat{x} + y_n\hat{y} + z_o\hat{z}|)$$

$$V_p(\vec{r}) = \sum_{mno} v_p(|x_m\hat{x} + y_n\hat{y} + z_o\hat{z}|)$$

$$x_m = x + mL_x, \quad y_n = y + nL_y, \cdots$$

The Algorithm

[1] Sample $|R,S\rangle$ initial walkers from $|\langle\Psi_T|R,S\rangle|^2$ using Metropolis Monte Carlo.

[2] We propagate in the usual diffusion Monte Carlo way with a drifted gaussian for half a time step.

[3] For each walker, we diagonalize the potential matrix.

[4] Loop over the eigenvectors, sampling the corresponding Hubbard-Stratonovich variable and update the spinors for half a time step. We use the expectation value of $\langle\Psi_T|\vec{\sigma}_i|R,S\rangle$ to introduce approximate importance sampling of the Hubbard-Stratonovich variables.

[5] Propagate the spin–orbit, using importance sampling

[6] Repeat 2, 3, 4 and 5 in the opposite order to produce a reversible propagator to lower the time step error.

[7] Combine all weight factors and evaluate new value of $\langle \Psi_T | R, S \rangle$. If the real part < 0 enforce constrained path by dropping the walker (keep it in the calculation of the mixed energy).

[8] Evaluate the averages of $\langle \Psi_T | R, S \rangle$, and $\langle \Psi_T | H | R, S \rangle$ to calculate the energy.

[9] Repeat as necessary.

Problems and Future plans

- Sign (phase) problem: construct trial functions with better nodal structure (backflow, sum of determinants,...); transient estimation

- Nuclei and nuclear matter: the tensor–isospin seem too strong. Our nuclear matter with tensor forces looks bad, whereas nuclear matter and ^{4}He with v_4 interactions are OK. It may be a problem of bad trial function.
  $\rightarrow$ Include Spin–orbit and three–body forces into our v_6 nuclear matter code

- Finite temperature : extend AFDMC ideas to Path Integral Monte Carlo

- Response functions: some recent ideas of Moroni and Baroni for sampling the path integral *polymer* using the classical reptation method may be useful.

4. - EOS of nucleon matter

Neutron Matter with v_8' +UIX

- We use the simplest trial function

$$|\Psi_T\rangle = \left[\prod_{i<j} f_{ij}^c\right] A \left[\prod_i |\phi_i, s_i>\right]$$

- The overlap is the determinant of the space-spin orbitals evaluated at the walker position and spinor for each particle multiplied by a central Jastrow product.

- For neutron matter in a box of side L, the orbitals are plane waves that fit in the box times up and down spinors.

- Usual closed shells are 2,14,38,54,66, ... particles.

Preliminary results of AFDMC calculations of the EOS of neutron matter with the Argonne v_8' two–body potential plus the Urbana IX three–body potential.

1. $AU8$ $\rightarrow$ Argonne v_8' + UIX

2. $AU6$ $\rightarrow$ Argonne v_6' + UIX

3. $A8$ $\rightarrow$ Argonne v_8'

4. $A6$ $\rightarrow$ Argonne v_6'

- AFDMC results for N=14,38,66 in a periodic box

- Results of PBFHNC calculations to estimate finite size corrections. Full FHNC for Jastrow correlations and two–body cluster for SOC correlation operators

- the correlation functions are computed by using FHNC/SOC theory

AU6 model with CBF theory[1]

Table 1: FHNC/SOC energy per particle of neutron matter for the $AU6$ interaction at various densities. T_F is the Fermi kinetic energy, and $< T >$ is the kinetic energy expectation value (average of the JF and PB kinetic energies). ΔE_2 is the second order perturbative correction. ΔE_{elem} is the contribution from the lowest order elementary diagram. All the quantities, except ρ/ρ_0, are expressed in MeV.

ρ/ρ_0	T_F	$< T >$	E_{FHNC}	ΔE_2	ΔE_{elem}
0.75	28.969	35.33	15.2	-0.9	0.6
1.00	35.094	43.82	20.4	-0.9	0.9
1.25	40.722	52.27	26.7	-1.5	1.2
2.0	55.708	74.40	54.8	-4.4	2.8
2.5	64.643	88.85	80.2	-6.1	3.8

[1] A.Fabrocini, private communication

AU8 model with FHNC/SOC

Table 2: FHNC/SOC energy per particle of neutron matter for the $AU8$ interaction obtained with a correlation operator of the type f_8, at various densities. T_F is the Fermi kinetic energy, and $< T >$ is the kinetic energy expectation value (average of the JF and PB kinetic energies). ΔE_{elem} is the contribution from the lowest order elementary diagram. All the quantities, except ρ/ρ_0, are expressed in MeV.

ρ/ρ_0	T_F	$< T >$	E_{FHNC}	ΔE_{elem}
0.75	28.969	36.55	12.8	0.5
1.00	35.094	45.79	16.7	0.9
1.25	40.722	54.41	21.7	1.3
2.0	55.708	78.83	44.5	3.0
2.5	64.643	95.10	67.2	4.5

AFDMC calculations with 14 neutrons

Table 3: AFDMC energies per particle in MeV of 14 neutrons in a periodic box for interaction models at various densities. Error bars for the last digit are shown in parentheses.

$\rho(fm^{-3})$	$A6$	$AU6$	$A8$	$AU8$
0.12	12.41(4)	14.96(6)	12.32(5)	14.80(9)
0.16	15.12(4)	19.73(5)	14.98(6)	19.76(6)
0.20	17.86(5)	25.29(6)	17.65(7)	25.13(8)
0.32	27.84(6)	48.27(9)	27.3(1)	48.4(1)
0.40	36.0(1)	69.9(1)	35.3(1)	70.3(2)

Table 4: AFDMC energies per particle in MeV for the $AU6$ and $AU8$ model interactions at various densities and for different numbers of neutrons. Error bars for the last digit of the Monte Carlo calculations are shown in parentheses.

Model	$\rho(fm^{-3})$	14	38	66
AU6	0.12	14.96(6)		14.93(4)
AU6	0.16	19.73(5)		
AU6	0.20	25.29(6)		26.51(6)
AU6	0.32	48.27(9)		53.1(1)
AU6	0.40	69.9(1)		79.4(1)
AU8	0.12	14.80(9)		
AU8	0.16	19.76(6)	18.7(1)	
AU8	0.20	25.23(8)		
AU8	0.32	48.4(1)	46.8(2)	54.3(6)
AU8	0.40	70.3(2)		

Spin–orbit problem

- SOC(6) $\rightarrow$ calcualtion with F_6
- SOC(8) $\rightarrow$ calcualtion with F_8

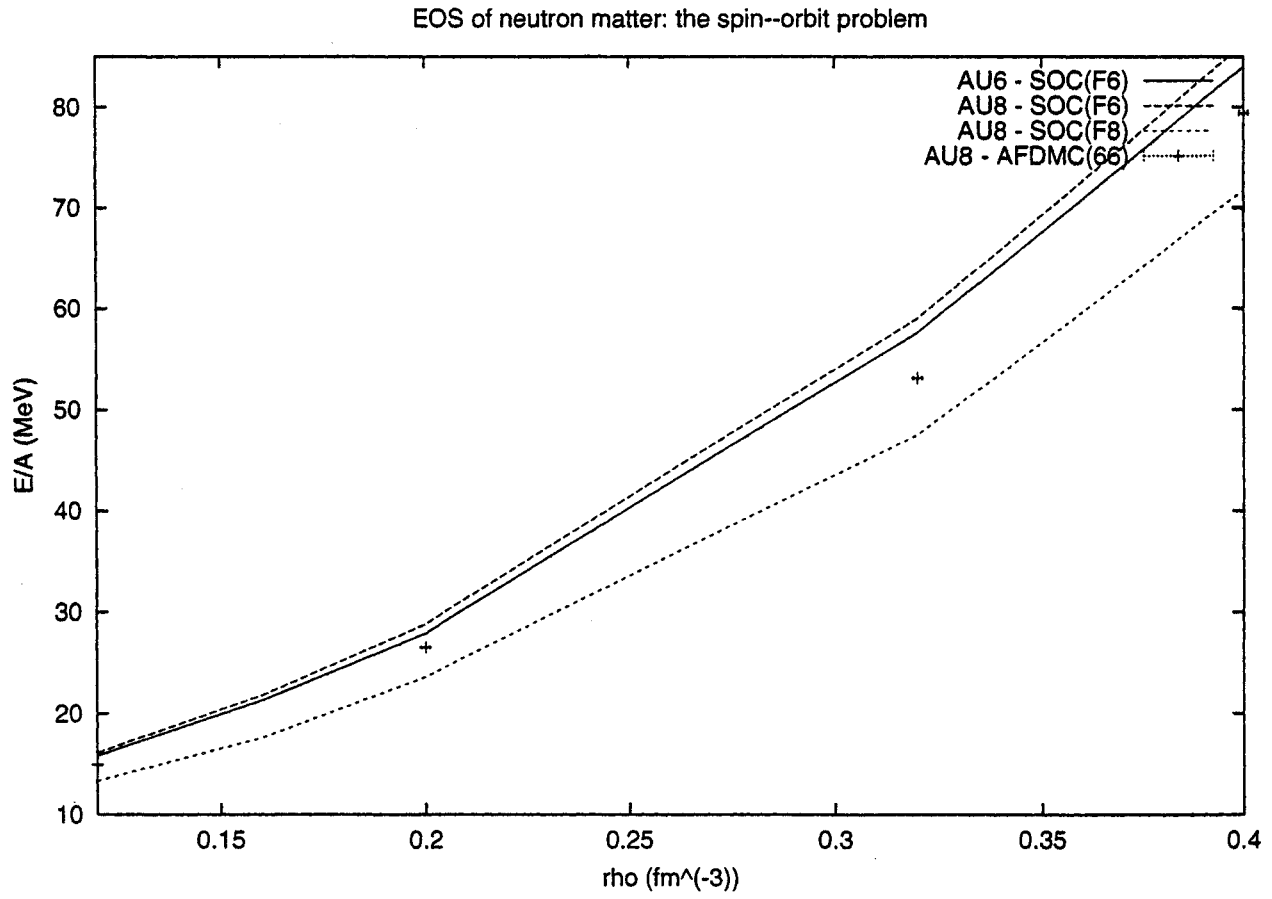

Neutron matter: a comparison of AFDMC with FHNC/SOC

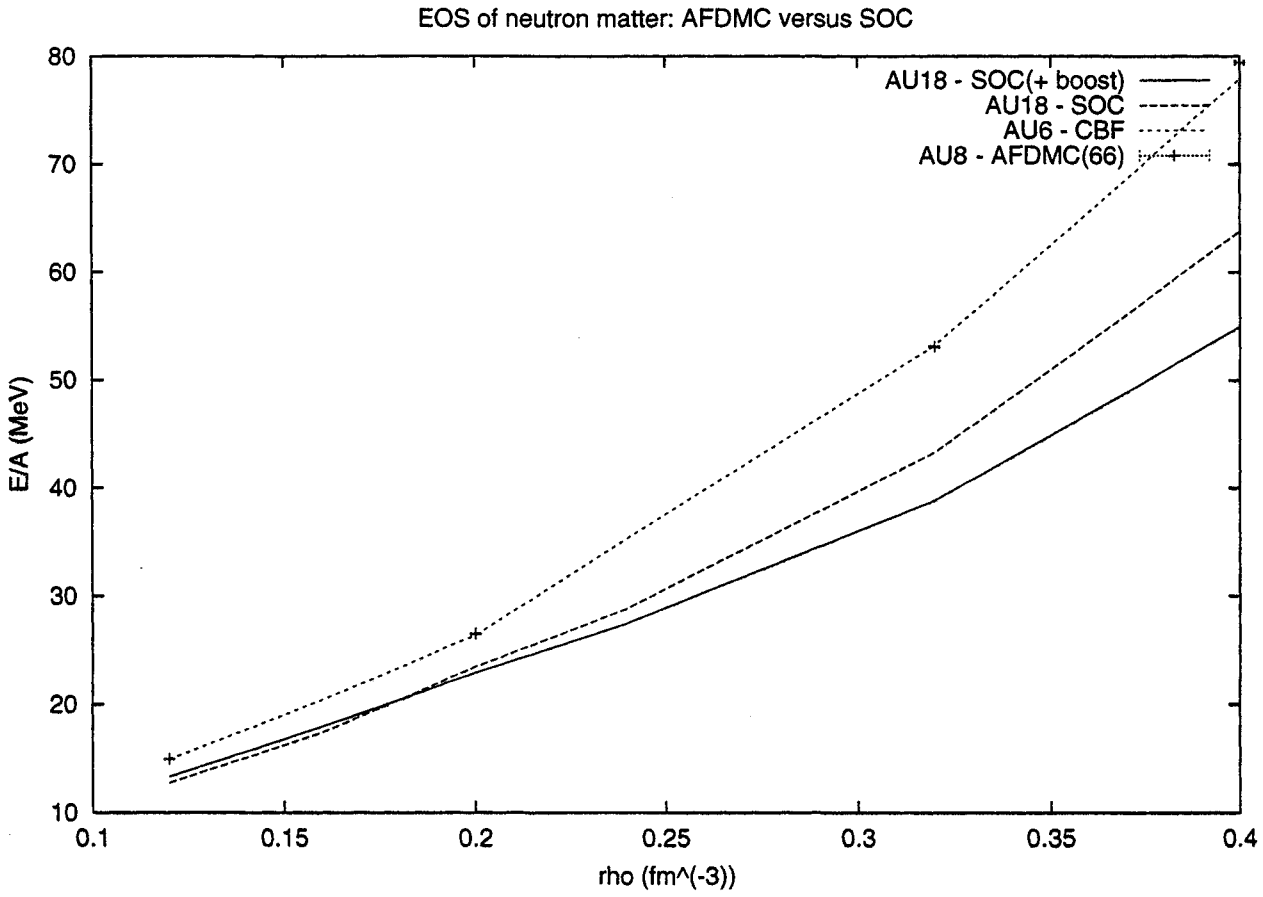

Compressibility of neutron matter

We have also calculated the compressibility $\mathcal{K}$ from the EOS of nuclear matter

$$\frac{1}{\mathcal{K}} = \rho^3 \frac{\partial^2 E_0(\rho)}{\partial \rho^2} + 2\rho^2 \frac{\partial E_0(\rho)}{\partial \rho} ,$$

$\rightarrow$ $E_0(\rho)$ is taken as a fit to the AFDMC energies
$\mathcal{K}_F = 9\pi^2 m/(k_f^5 \hbar^2)$ $\rightarrow$ Fermi gas the compressibility

$$\frac{\mathcal{K}}{\mathcal{K}_F} = \frac{1 + \frac{1}{3}F_1}{1 + F_0} ,$$

AFDMC and other calculations

(i) CBF $\rightarrow$ from EOS; (ii) AU18[2] $\rightarrow$ from EOS; (iii) Reid6[3]$\rightarrow$ from Landau parameters ; (iv) Reid[4] $\rightarrow$ from Landau parameters

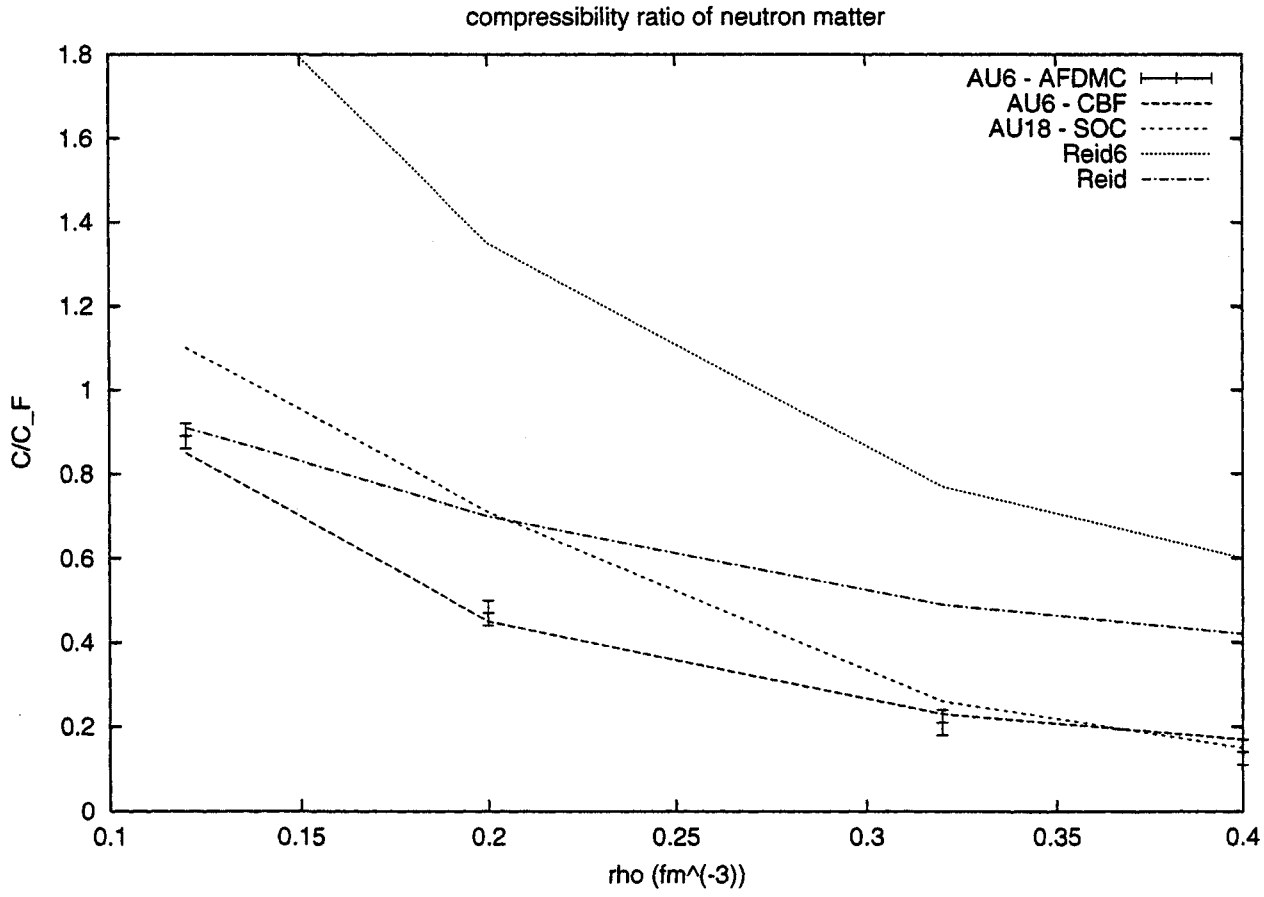

[2]A.Akmal et al., Phys. Rev.**C58** (1998) 1804

[3]A.D.Jackson et al., Nucl. Phys. **A386** (1992) 125

[4]S.O.Backman et al., Phys. Lett. B43(1973) 263

Nuclear matter with AFDMC[1]

We have computed (i) ^{4}He nucleus, (ii) symetrical and (iii) asymmetrical nuclear matter with v_4 type of two–body interactions

- Argonne v_4' two–body potential
- Modified S3 (MS3) potential by Afnan and Tang[2]. As in other calculations, we have added an interaction for the odd channels, given by the repulsive term of the even channels.

V(r) used for the mean field part of Ψ_T

$$V(r) = \frac{V_0}{1 + \exp(\frac{r-R}{a})}$$

$\rightarrow \quad V_0 = -56.2MeV$, $R = 1.8fm$ and $a = 0.22fm$

[1] S.Fantoni, A.Sarsa and K.E.Schmidt, in *Adv. in Quantum Many-body Theories*, in press

[2] I.R.Afnan and Y.C.Tang, Phys.Rev. **175** (1868) 1337

v_4 model of Nuclear matter with PBFHNC[3], FHNC/SOC and Auxiliary Field DMC

Table 1: Results for the v_4' model of symmetrical nuclear matter at $\rho = 0.16$.The AFDMC column reports the mixed energy at a time step of $5 \times 10^{-5}\mathrm{MeV}^{-1}$. The PBFHNC and the FHNC/SOC results refer to the Jackson–Feenberg energy. PB-FHNC is calculated with the F_1 trial function and FHNC/SOC with the F_4. The PBFHNC and FHNC/SOC results should be corrected by adding $+0.6MeV$ which corresponds to the contribution from the elementary diagram E_0. The number in parenthesis for AFDMC gives the statistical error. The energies per particle are in MeV.

A	$PBFHNC$	$FHNC/SOC$	$AFDMC$
28	1.30	-	0.34(3)
2060	1.95	-	↓
∞	1.92	1.45	0.96

[3]S.Fantoni and K.E.Schmidt, Nucl. Phys. **A690** (2001) 456

Table 2: Results for the MS3 model of symmetrical nuclear matter at $\rho = 0.16$. The PBFHNC and FHNC/SOC results should be corrected by adding $+1.2MeV$ which corresponds to the contribution from the elementary diagram E_0.

A	$PB-FHNC$	$FHNC/SOC$	$AFDMC$
28	-14.79	-	-16.17(6)
76	-16.83	-	-18.08(3)
2060	-15.15	-	$\downarrow$
∞	-15.20	-16.10	-16.5

Table 3: Time step dependence of AFDMC calculations for the MS3 model of asymmetrical nuclear matter at $\rho = 0.16$. The energies per particle are in MeV. The time step $\Delta\tau$ is in units $10^{-5}\mathrm{MeV}^{-1}$)

N	Z	α	$\Delta\tau$	$E(N,Z)$	ΔT_{free}
14	2	0.75	10	5.52(4)	0.69
14	2	0.75	5	5.55(5)	0.69
38	14	0.46	10	-8.69(6)	0.77
38	14	0.46	5	-8.79(5)	0.77

v_4 model of neutron matter

Table 4: Results for the MS3 model of pure neutron matter at $\rho = 0.16$. The PBFHNC and FHNC/SOC results should be corrected by adding $+2.2MeV$ which corresponds to the contribution from the elementary diagram E_0.

N	$PB-FHNC$	$FHNC/SOC$	$AFDMC$
14	24.42	-	25.46(2)
38	22.49	-	23.15(1)
66	24.30	-	24.80(1)
1030	24.79	-	$\downarrow$
∞	24.72	24.49	25.4

MS3 model of asymmetric matter

- dashed : FHNC/SOC with elementary diagram E_0
- solid : FHNC/SOC without elementary diagrams
- asymmetry coefficient with AFDMC: $a_\tau \sim 37 MeV$

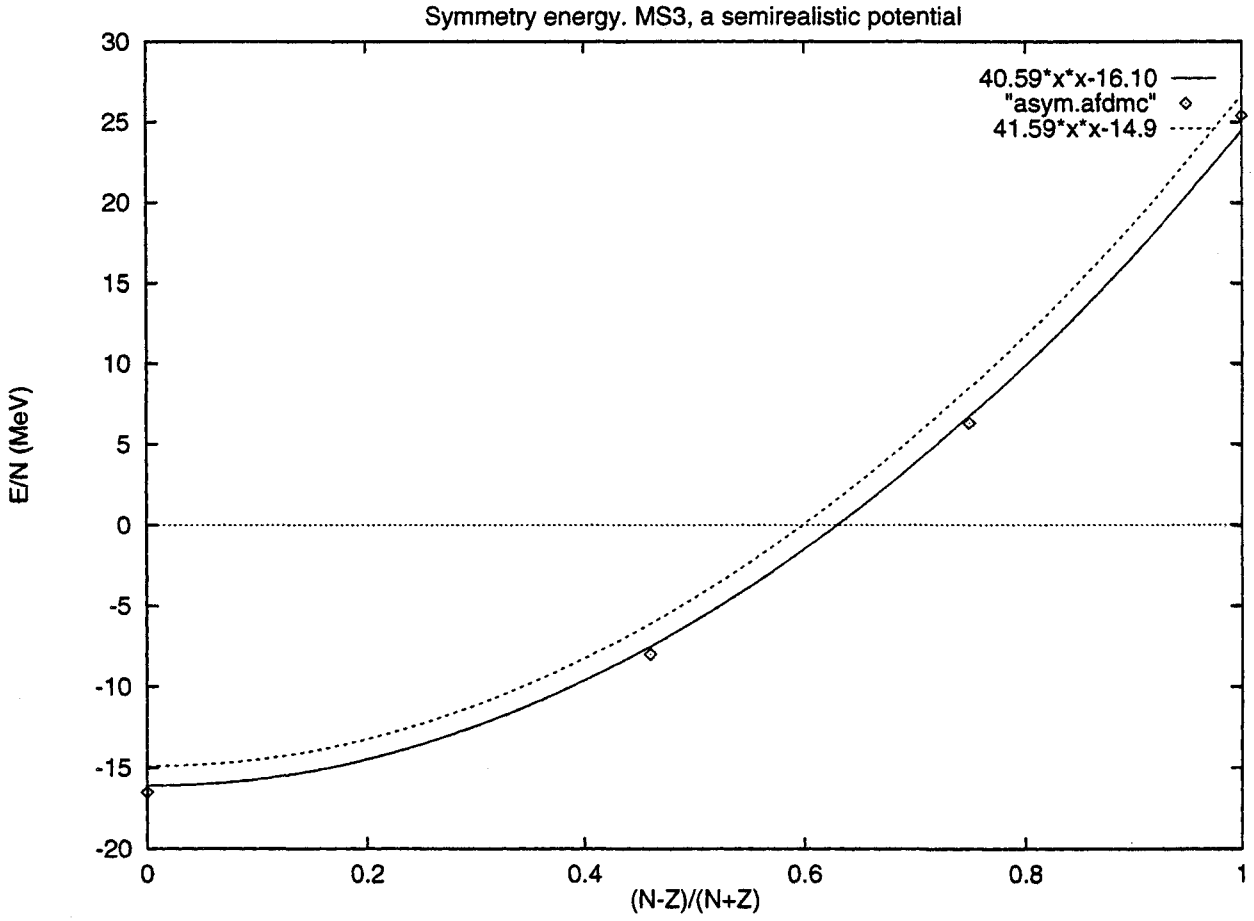

MS3 model of the Alpha particle with AFDMC, VMC[4], Hyperspherical Harmonics[5] and Coupled Cluster[6]

Table 5: AFDMC results for the MS3 model of the alpha particle, compared with the variational Monte Carlo (JLO), Hyperspherical Harmonics (HH) and the Coupled Cluster (TICC[2]-SD) results. In parenthesis is given the statistical error.

Method	$\Delta\tau(10^{-5}\mathrm{MeV}^{-1})$	$E(\mathrm{MeV})$
JLO	-	-30.41(2)
HM	-	-30.299
TICC[2]-SD	-	-28.21
AFDMC	1	-29.95(7)
AFDMC	2	-29.42(6)
AFDMC	3	-29.28(6)

[4]E.Buendia et al., J. Phys. G: Nucl.Part. Phys., 2001

[5]S.Rosati et al. in *Adv. in Quantum Many-body theories* **2**, *2001*

[6]Navarro, lectures at this school

5. - Neutron Droplets[1]

We compare to the 7 and 8 Neutron droplet calculations using GFMC and the v18+UIX interaction[2]

Their purpose was to improve Skyrme models.

Since these small neutron clusters are not bound, they added an external potential.

$$V_{\rm external}(r) = \frac{V_0}{1+\exp\left(\frac{r-R}{a}\right)}$$

with

$$\begin{aligned} V_0 &= -20\,{\rm MeV} \\ R &= 3\,{\rm fm} \\ a &= 0.65\,{\rm fm} \end{aligned}$$

---

[1] In collaboration with J. Carlson and F. Pederiva

[2] B.S. Pudliner, A. Smerzi, J. Carlson, V.R. Pandharipande, Steven C. Pieper, and D.G. Ravenhall, Phys. Rev. Lett. **76**, 2416 (1996)

Neutron Droplet Results

A	$\Delta\tau$	Energy	Growth Energy
8	5.0×10^{-5}	-36.8(2)	-36.2(3)
7	5.0×10^{-5}	-30.0(2)	-29.0(3)

8 neutron GFMC result is -37.6(3) MeV.
7 neutron J=1/2 GFMC result is -32.3(2) MeV.
7 neutron J=3/2 GFMC result is -31.2(2) MeV.

The reported differences between v8' and v18 are less than 0.2 MeV for the GFMC calculations. Their best variational wave function gave -35.6(1) MeV for 8 particles. Our central variational wave function gives an energy of -25.8(4) MeV.

Our 7 neutron results used a closed shell trial function with a neutron removed from a spin up $p_x - p_y$ space orbital. This required no change to the code but the trial function does not have good angular momentum.

6. - Spin susceptibility of neutron matter[1]

AFDMC calculations show that strong correlations induced by modern nucleon interactions lead to a sizable reduction of χ.

χ and the neutrino mean free path

- effects due to strong interactions are relevant, in the spin-density channel which couples with the axial vector current.

- small χ's (or big G_0's) $\rightarrow$ suppression of the Gamow–Teller transitions.

- need of the spin response at zero and finite temperature in a wide range of densities

[1] S.Fantoni, A.Sarsa and K.E.Schmidt, Phys. Rev. Lett., in press

Theoretical calculations of χ

- no calculations of χ with modern potentials; previous evaluations of Landau parameters were based either on Skyrme–type potential models or on semirealistic interactions.

- theoretical estimates of χ/χ_F may differ up to a factor 3 at ρ_0, and even more at higher densities.

- need of *ab initio* calculations with modern many–body methods to compute χ

Skyrme models :
small values of G_0
instabilities for densities in the range $(2-4)\rho_0$

Microscopic calculations :
Reid or Bethe–Johnston potentials
convergence and/or spin problem

The actual calculation

The Hamiltonian we have considered to compute the spin susceptibility in a magnetic field, ignoring any orbital effects, is given by

$$H = H_0 - \sum_i \vec{\sigma}_i \cdot \vec{b}$$

where

$$\begin{aligned} \vec{b} &= \mu \vec{B} \\ \mu &= 6.03 \times 10^{-18} \mathrm{MeV/Gauss} \end{aligned}$$

We have computed the susceptibility according to its definition

$$\chi = -\rho \mu^2 \frac{\partial^2 E_0(b)}{\partial b^2}\bigg|_{b=0}$$

$E_0(b)$ is the ground energy in field b.

The Pauli expansion

Pauli expansion of the energy per particle as a function of the spin polarization $p = -\partial E_0(b)/\partial b|_{b=0}$:

$$E(p) = E(0) - b\ p + \frac{1}{2}p^2 \frac{\partial^2 E}{\partial p^2}|_0$$

Minimize $E(p)$ with respect to p

$$\chi = \mu^2 \rho \left(\frac{\partial^2 E}{\partial p^2}|_0 \right)^{-1}$$

Fermi gas susceptibility $\chi_F \to \mu^2 m k_f/(\hbar^2 \pi^2)$.

AFDMC calculation

AFDMC gives the energy eigenvalue, $E_0(J_z, b)$, for the interacting system in a field b:

- finite number of neutrons in a periodic box
- quantum state of a given spin asymmetry $J_z = N_\uparrow - N_\downarrow$.

Assuming that the energy and polarization are known in terms of J_z, use chain rule

$$\frac{\partial^2 E}{\partial p^2}|_0 = \left[\frac{\partial p}{\partial J_z}\right]^{-2} \left\{ \frac{\partial^2 E_0}{\partial J_z^2} - \frac{\partial E_0}{\partial J_z} \left[\frac{\partial p}{\partial J_z}\right]^{-1} \frac{\partial^2 p}{\partial J_z^2} \right\}$$

Since we are calculating the lowest energy state, the derivative of the energy with respect to J_z vanishes:

$$\frac{\partial^2 E}{\partial p^2}|_0 = \left[\frac{\partial p}{\partial J_z}\right]^{-2} \frac{\partial^2 E_0}{\partial J_z^2}$$

Non–interacting finite systems

The energy is not a quadratic function of the external field b.

- consider different $(N_\uparrow, N_\downarrow)$ systems with $N \sim 60$
- each of the $E_0(J_z, b)$ is tangent to the Pauli parabola
- the Pauli parabola agrees with the exact Fermi gas up to about $b \sim 50MeV$
- one gets $\chi/\chi_F \sim 1$ for $J_z = 50$ and $J_z = 57$

Table 1: Closed shells which correspond to about 60 particles.

J_z	$N_\uparrow$	$N_\downarrow$	N
0	33	33	66
6	33	27	60
50	57	7	64
57	57	0	57

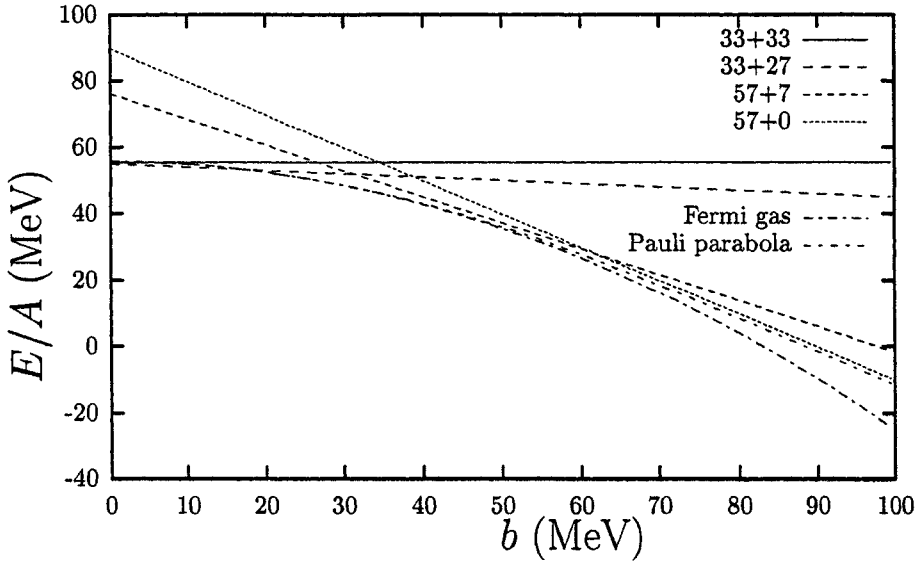

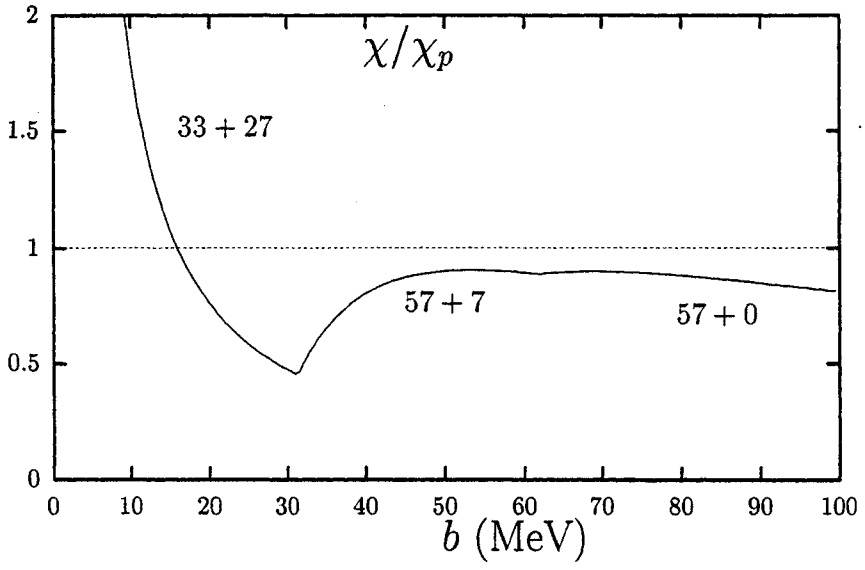

The interacting case

In the interacting case, the derivatives of the polarization and of the energy with respect to J_z can be easily estimated by using the following equations

$$\frac{\partial p}{\partial J_z} \approx \frac{E_0(J_z = J_{z0}, b = 0) - E_0(J_z = J_{z0}, b = b_0)}{J_{z0}\ b_0}$$

$$\frac{\partial^2 E_0}{\partial J_z^2} \approx 2\,\frac{E_0(J_z = J_{z0}, b = 0) - E_0(J_z = 0, b = 0)}{J_{z0}^2}$$

based on the following assumptions

- for $b = 0$, $E_0(J_z, b)$ is quadratic in J_z;
- for a fixed J_z, $E_0(J_z, b)$ is linear in b;
- the polarization is linear in J_z (in the non interacting case $p = J_z/N$) .

Our optimal values, based on the non–interacting case analysis :

$$\begin{aligned} J_{z0} &= 50 \\ b_0(\rho = 0.12) &= 28 \\ b_0(\rho = 0.20) &= 39 \\ b_0(\rho = 0.32) &= 53 \\ b_0(\rho = 0.40) &= 62 \end{aligned}$$

- we have verified the dependence of χ/χ_F on J_{z0}, performing simulations with $J_{z0} = 6$ and found that it is very weak

- we have verified the linearity of $E(J_{z0} = 50, b)$ on b beyond $b_0 = 39MeV$ and found that χ/χ_F is largely independent on b_o.

Spin susceptibility of neutron matter

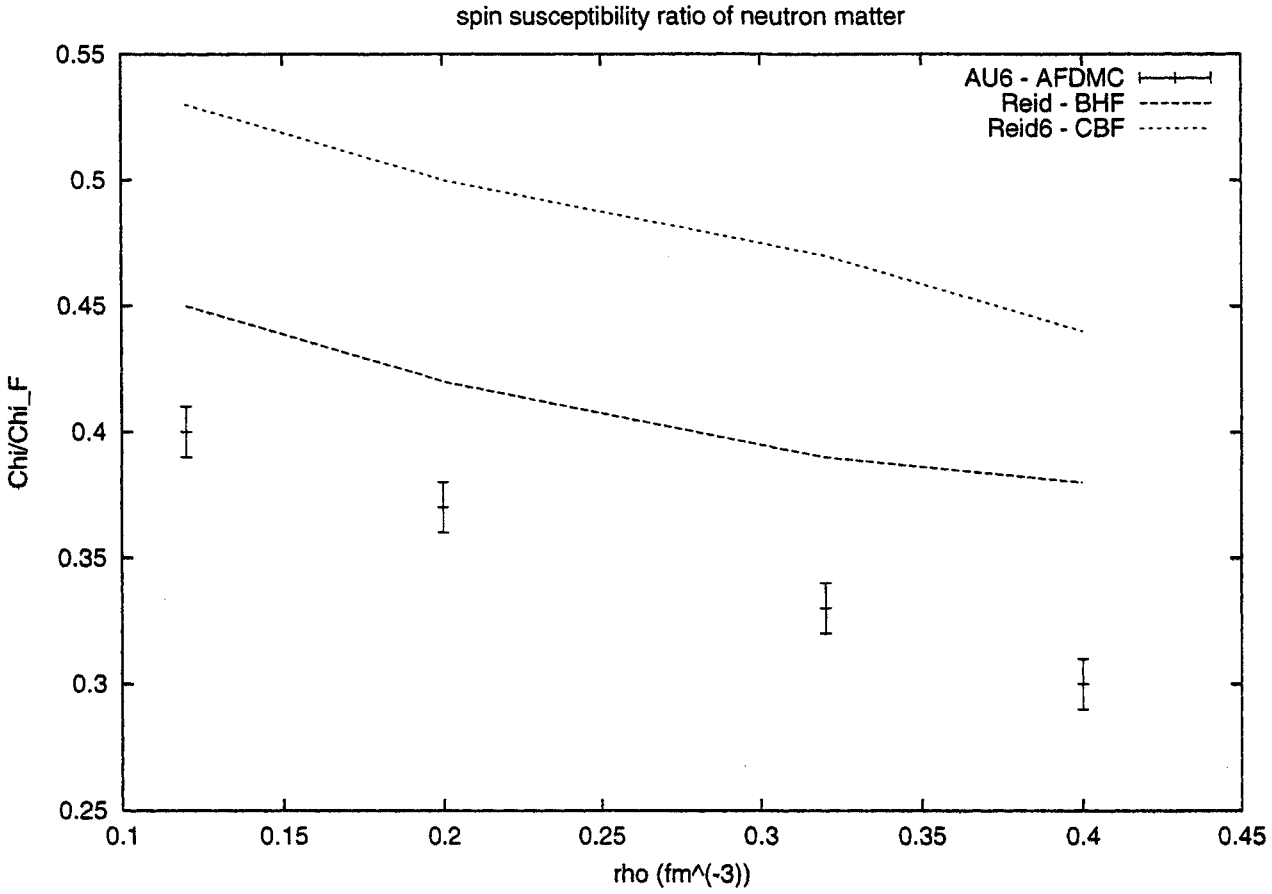

Discussion of the results

- $AU6$ and $AU8$ give the same results within statistics

- The AFDMC result for χ/χ_F is $0.36(1)$ with Reid6 at $\rho = 0.20 fm^{-3}$ is $0.36(1)$
  $\rightarrow$ compare with 0.50 obtained by CBF theory[2]

- Jackson et al. (Reid6) and S.Backman et al (Reid)[3] compute the Landau parameters, and not directly χ/χ_F

- a time step $\Delta\tau = 10^{-4} MeV^{-1}$ was sufficient in most of the quantum simulations to obtain agreement between the mixed and the growth energies within the statistical accuracy.

- finite size effects have been estimated to give less than 10% contribution.

[2] Jackson et al., Nucl. Phys. **A386** (1982) 125
[3] S.Backman et al., Phys. Lett. **43B** (1973) 263

Multipair contributions

The results given in the figure for Reid6 and Reid (S.Backman et al, Phys. Lett. **43B** (1973) 263) are obtained from

$$\frac{\chi}{\chi_F} = \frac{1 + \frac{1}{3}F_1}{1 + G_0}$$

instead of

$$\frac{\chi}{\chi_F} = \frac{m^\star}{m} \frac{|\eta|^2}{1 + G_0 - iO(H^2)} + \frac{\chi_M}{\chi_F} \ ,$$

$\rightarrow$ η the renormalization of quasiparticle spin
$\rightarrow$ the $O(H^2)$ term is the tensor contribution to the Landau parameter
$\rightarrow$ χ_M/χ_0 is the multipair contribution to the response.

7. - Conclusions and Future Plans

- AFDMC opens up a new generation of fully microscopic calculations for nuclear systems, at normal and high density.

- AFDMC allows for $N \neq Z$, as well as for spin polarized systems

- Simulations already done up to 76 nucleons with modern potentials

- The spin susceptibility of neutron matter between ρ_0 and $2\rho_0$ is one third of the Pauli susceptibility.

- The neutron matter EOS reasonable agree with FHNC/SOC, except for a possible spin–orbit problem. Three–body interaction.

- ^{4}He, symmetric and asymmetric nuclear matter with v_4 interactions.

Future Plans

1. Complete study of v_8+UIX neutrons

2. Neutron Drops – complete calculation of A=7 and 8 neutron drops

3. Transient Estimation

4. Backflow correlation (spin–orbit and tensor–τ)

5. Nuclei and Nuclear Matter with realistic interactionsa

6. Finite temperature

7. Response functions

8. Mesons, Nucleons, and Deltas